1 Gene duplication at the Fascicled earl locus controls the fate of

2 inflorescence meristem cells in maize

- 3 Yanfang Du^{a,b,1}, China Lunde^{b,1}, Yunfu Li^{a,1}, David Jackson^{c,a}, Sarah Hake^{b,2}, Zuxin Zhang^{a,2}
- 4 a National Key Laboratory of Crop Genetic Improvement, Huazhong Agricultural University, Wuhan
- 5 430070, P.R. China
- 6 b Plant Gene Expression Center, USDA-ARS and UC Berkeley, Albany, California 94710
- 7 c Cold Spring Harbor Laboratory, Cold Spring Harbor, NY 11724
- 8 1 These authors contributed equally to this work.
- 9 2 Address correspondence to hake@berkeley.edu or zuxinzhang@mail.hzau.edu.cn.

10 Classification: Biological Sciences; Developmental Biology;

- 11 **Keywords**: Maize (*Zea mays* ssp. *mays*.); inflorescence meristem; fascicled
- inflorescence; gene duplications; central/peripheral

13 Author Contributions

- 14 Z.Z., C.L. and S.H. designed research; Y.D., C.L., Y.L. and D.J. performed research;
- 15 Y.D., C.L. and Y.L. analyzed data; Y.D., C.L., S.H. and Z.Z. wrote the paper; S.H. and
- 16 Z.Z supervised research.

17

18 This PDF file includes:

- 19 Main Text
- Figures 1 to 5
- 21 Supplemental materials (5 figures and 5 tables)

Abstract

Plant meristems are self-renewing groups of pluripotent stem cells that produce lateral organs in a stereotypical pattern. Of interest is how the radially symmetrical meristem produces laminar lateral organs. Both the male and female inflorescence meristems of the dominant Fascicled ear (Fas1) mutant fail to grow as a single point and instead show deep branching. Positional cloning of two independent Fas1 alleles identified a ~160 kb region containing two floral genes, the MADS-box gene zmm8 and the YABBY gene drooping leaf2 (drl2). Both genes are duplicated within the Fas1 locus and spatiotemporally misexpressed in the mutant inflorescence meristems. Increased zmm8 expression alone does not affect inflorescence development; however, combined misexpression of zmm8, drl2 and their syntenic paralogs zmm14 and drl1, perturbs meristem organization. We hypothesize that misexpression of the floral genes in the inflorescence and their potential interaction cause ectopic activation of a laminar program, thereby disrupting signaling necessary for maintenance of radially symmetrical inflorescence meristems. Consistent with this hypothesis, RNA sequencing and *in situ* analysis reveal altered expression patterns of genes that define distinct zones of the meristem and developing leaf. Our findings highlight the importance of strict spatiotemporal patterns of expression for both zmm8 and drl2 and provide an example of novel phenotypes arising from tandem gene duplications.

Significance Statement

The maize ear is unbranched and terminates in a single point. The ear and tassel inflorescences of *Fascicled ear* mutants fail to grow as a single point and instead are branched. This phenotype results from the temporal misexpression of duplicated transcription factors, ZMM8 and DRL2. We hypothesize that these gene rearrangements create novel promoters or regulatory sequences that cause misexpression at the inflorescence transition stage thus activating a laminar program, ablating the meristem and producing branches. The work demonstrates that *zmm8* and *drl2* must be restricted from the inflorescence meristem to maintain its terminal point and conversely, a mechanism by which branching may be imposed. Manipulation of these genes can be used to alter tassel and ear architecture, potentially to improve agronomic traits.

Main Text

Introduction

Plant architecture results from the activities of meristems, groups of totipotent cells that maintain a central population of indeterminate cells while initiating organs peripherally. The types of organs formed by the meristem depend on whether the plant is in its vegetative or reproductive phase. Leaves form during the vegetative phase, subtending suppressed axillary meristems. However, in the reproductive phase, leaves are reduced, and axillary meristems predominate, producing branches or flowers, depending on the species (1).

Meristems are radially symmetrical with a central/peripheral axis. During initiation of determinate lateral organs of the shoot, including leaves and floral organs, radial symmetry is broken with the onset of asymmetric patterning (2). The localized planar growth of lateral organs is derived from their positional relationship to the meristem (3–5) in which the adaxial surface faces the meristem while the abaxial surface faces away from the meristem (2). Thus, the central/peripheral axis continues into the adaxial/abaxial axis of shoot lateral organs (2).

 Laminar outgrowth of lateral organs results from boundaries created by the juxtaposition of cells expressing antagonistic abaxial and adaxial fate regulatory factors (6,7). This same juxtaposition exists within the radial shoot axis, with adaxial genes expressed in the center and abaxial genes expressed in the periphery (8). Abaxial genes are excluded from the center of the meristem (9–11). The genetic basis of polarity establishment in Arabidopsis involves several distinct transcription factor families and small regulatory RNAs (12). The CLASS III Homeodomain-Leucine Zipper (HD-ZIPIII) family is responsible for adaxial cell fate; *KANADI* and *YABBY* gene families, Auxin Response Factors (*ARF3* and *ARF4*), together with the miRNA *miR166*, all contribute to abaxial cell fate identity in Arabidopsis (13,14).

Multiple levels of regulation exist to maintain the meristem so that it is not consumed in organogenesis nor increased in size beyond what is needed for growth of the plant. The well-studied pathway for meristem maintenance is the CLAVATA3 (CLV3)-WUSCHEL (WUS) negative feedback loop, through which the balance of stem cell fate occurs as WUS activates *CLV3* expression and the CLV3 signal is transmitted to the central domain to restrict the expression of *WUS*, through LRR receptors CLV1 and CLV2 (15–17). The CLV-WUS pathway is well-conserved (16), and mutant phenotypes have been described for maize orthologs of *CLV1*, *CLV2* and *CLV3* (17–20). Maize contains two distinct inflorescence meristems (IMs): the apical male tassel, and the lateral female ear, which forms in the axil of a leaf (21). The loss-of-function *CLV* phenotypes include enlarged inflorescence meristems with both fasciated tassels and ears due to interference with regulation of IM development (17–20).

Fascicled ear1 (Fas1), is a dominant maize mutant, displaying reiterated bifurcation of both the tassel and ear (22). Fascicled, which means bundled or bunched in Latin, distinguishes Fas1 from the large class of fasciated ear mutants that are not branched. Here, we describe positional cloning and analysis of the Fas1 locus. A tandem duplication of the Zea mays MADS8/drooping leaf2 (zmm8/drl2) gene pair causes the dominant Fas1 phenotype through spatiotemporal mis-regulation of both genes. Genes that regulate central/peripheral zone cell fates are differentially expressed. We propose a model where early misexpression of zmm8/drl2 in the IMs affects the regulation of central/peripheral zone identity, leading to punctate domains of meristem termination followed by ectopic proliferation of lateral domain cells, resulting in repeated bifurcation of male and female

IMs. These data indicate that maintenance of central/peripheral identity is required within cells of the IM to sustain its single, terminal central axis.

Results

Fas1 is a dominant mutation with repeated bifurcation in the tassel and ear

Fascicled ear1 (Fas1) mutants were discovered as naturally occurring mutations in two separate breeding lines: Fas1-R (23) and Fas1-2. The Fas1 mutation affects both male and female inflorescences and has no effect on vegetative plant architecture. Mutants fail to maintain a single terminal IM and instead display deep branching caused by continuous bifurcations along the axis of the rachis (Fig. 1A-D). In Fas1-2 in the B73 inbred background, the tassel lacks a central rachis, resulting in many long branches (Fig. 1A, 1E, and SI Appendix, Table S1). Fas1-R tassels in either the A188 or B73 inbred backgrounds, display a central rachis that splits several times leading to multiple terminal points instead of one (ranging from 2 to 6) (Fig.1B, 1F, and SI Appendix, Table S1). Whereas normal ears are unbranched, Fas1-2 ears undergo two or three bifurcations but maintain normal kernel development (Fig.1C, 1G, and SI Appendix, Table S2). Fas1-R ears show variable bifurcation numbers leading to many terminal points (Fig.1D, 1H, and SI Appendix, Table S2). Tassel length and tassel branch number show no dosage effects, but kernel row number and length-width ratio of the ear are intermediate in heterozygotes (SI Appendix, Table S1-S2).

Scanning electron microscopy reveals initial events that lead to bifurcation

To better understand early inflorescence organogenesis in Fas1-2 and Fas1-R mutants, young (1-2 mm) ears and tassels were visualized using scanning electron microscopy (SEM). In wild type of all genetic backgrounds, after the transition from vegetative meristem to the IM, the tassel and ear IMs initiate SPMs, which each initiate two spikelet meristems (SMs), that in turn initiate two FMs (Fig. 2A-F). Throughout development, the IM maintains a single organizing center, terminating in a single tassel rachis or ear tip.

In the early stage of Fas1-2 ear (B73) development, the IM becomes wider and the peripheral region grows while the central region ceases. Two or three independent ear-like structures arise. Each newly formed IM initiates a normal progression of SPMs, SMs and FMs (Fig. 2G-J); In A188, the Fas1-R ear IM displays line fasciation and undergoes repeated rounds of bifurcations leading to multiple branch-like structures. Spikelet primordia initiate normally on the abaxial surface of each new structure, but the adaxial surfaces lack spikelet primordia (Fig. 2K-O).

In the early stage of Fas1-2 tassel (B73) development, primordia initiate from the apical surface, leading to a loss of growth of the tassel rachis as cells are recruited to new primordia that develop into branch-like structures with normal spikelets (Fig. 2P-S). Fas1-R tassels in A188 are slightly different. At first, the IM enlarges while initiating normal branches, then the center of the apical meristem halts while the peripheral region fasciates

to form a flat meristem with a deep central depression. The fasciated meristem then splits into many branched structures (Fig. 2*T-W*).

In both alleles at this early stage, male and female inflorescences share a common phenotype. Growth of the central region is repressed and peripheral zone growth is promoted, forming inflorescences with deep branching. Fas1-2 and Fas1-R differ in that the bifurcations persist longer in Fas1-R ears and sometimes lead to secondary axes in which the adaxial side lacks spikelets.

Duplication of both zmm8 and drl2 cause fascicled inflorescences

143

144

145146

147

148

160

161

162

163

164

165

166

167

168 169

170

171

172

173174

175

176177

178

179

Fas1-R was first mapped on the long arm of chromosome 9 using the standard set of waxy 149 reciprocal translocations (24). The final mapping region was narrowed to 167 kb located 150 151 in bin 9.06 between IDP580 and custom marker SSR10 using 426 individuals (SI Appendix, 152 Fig. S1). Fas1-2 was mapped in a B73 F₂ population using Bulked-Segregant RNA sequencing with 30 1-2 cm ears of Fas1-2 and a similar pool of normal siblings, followed 153 by fine-mapping with 7,680 F_2 individuals. The mapping region was narrowed to ~160 kb, 154 between marker BMC5 and BMC6 on chromosome 9, which showed a consistent mapping 155 region with Fas1-R (Fig. 3A and SI Appendix, Fig. S1). (Mapping primers are listed in SI 156 157 Appendix, Table S3.) In B73, two genes reside in this interval, the MADS-box gene zmm8 (Zm00001d048082) and the YABBY gene drooping leaf2 (drl2, Zm00001d048083) (Fig. 158 159 3A).

We carried out a revertant screen of Fas1-R and identified two revertants in 3,378 plants. The high frequency of reversion suggested the possibility of gene duplication at the Fas1 locus. To determine if there was copy number variation at the Fas1 locus, we performed restriction fragment length analysis using DNA blots with specific probes located within zmm8 and drl2. Genomic DNA digested with HindIII followed by blotting with zmm8specific Probe1, shows one specific band of 7,433 bp in B73 and the normal sibling, consistent with B73 RefGen v4 (Fig. 3B-C). In Fas1-2 and Fas1-R, however, the 7,433 bp band has higher intensity, and there is an additional band of ~4.4 kb. When digested with XbaI and hybridized with zmm8-specific Probe1, the normal individuals show the expected size band, but the mutants have two bands of different sizes (Fig. 3C). Sequence analysis confirmed that the difference in band number was not due to novel XbaI sites within the region of zmm8-specific Probe1 in Fas1 mutants. The lower band in Fas1-R is of higher intensity suggesting an increase in copy number (Fig. 3C). These results suggest that there could be two copies of zmm8 in Fas1-2, but two or more copies in Fas1-R. Consistent with the possibility of copy number variation, one of the revertants, Fas1-Rev2, lost one of the extra copies of zmm8.

With the *drl2*-specific Probe2, one band is identified in B73 and the normal sibling after digestion of genomic DNA with *XbaI* or *NcoI*. The sizes are consistent with B73 RefGen_v4 (5,674 bp for *XbaI* and 1,3847 bp for *NcoI*) (Fig. 3*B-C*). Two different bands are found in *Fas1-2* and *Fas1-R* for each enzyme, and the lower band is more intense only

in Fas1-R and its derivative revertant alleles (Fig. 3C). These results support the hypothesis that there are two copies of drl2 in Fas1-2, but two or more copies in Fas1-R. However, unlike the results with the zmm8 probe, neither revertant showed any differences compared to the Fas1-R drl2-specific Probe2 banding pattern. Taken together, based on the copy number changes and available sequence, a possible arrangement of zmm8 and drl2 in Fas1-2 and Fas1-R is shown in Fig. 3D. Fas1-2 and Fas1-R are independent alleles, which contain two or more duplicated copies. The extra copies are tightly linked in both alleles.

In order to assess whether the duplication found in the Fas1 alleles was unique, we compared our contiguous genomic sequence from Fas1-2 containing zmm8, the intergenic region, and drl2 to the recently released maize genomes (https://nam-genomes.org) using BLAST (25). The contiguous genomic sequence of Fas1-2 shares 99.92% sequence identity with the inbred B97. Remarkably, B97 has two copies of zmm8 (here referred to as zmm8-L and zmm8-R) and two copies of drl2 (referred to as drl2-L and drl2-R) at the syntenic region. Another inbred, Oh43, has one copy of drl2, but an extra truncated copy of zmm8 in addition to a full length copy of zmm8 (SI Appendix, Fig. S2 A).

To further study the gene duplications in B97 and Oh43, we compared the DNA blotting pattern between B73, Fas1-2, Fas1-R, B97 and Oh43 using zmm8-specific Probe1. Because of the similarity of zmm8 duplications in B97, two near equal-length bands were produced when digested with EcoRI (11,712 bp and 11,706 bp) or HindIII (7,450 bp and 7,456 bp), and each was slightly bigger than in B73 (SI Appendix, Fig. S2 A-B). Using a HindIII digestion, Fas1-2 and Fas1-R produced an additional band of a different size (SI Appendix, Fig. S2 A-B). These results show that Fas1-2 and Fas1-R have more zmm8 copies than B97. Additional sequence variation exists between B97 and the Fas1 alleles in the introns and intergenic region (SI Appendix, Fig. S2 C). Although copy number variation of zmm8 and dr12 exists in both B97 and Oh43, inflorescences of these two lines are normal, unlike Fas1 mutants.

zmm8 and drl2 are misexpressed at meristematic regions of Fas1 immature ear

To understand how the extra gene copies might affect expression patterns, we carried out quantitative RNA studies of *zmm8* and *drl2* in immature inflorescences. Compared to the wild type, *zmm8* was misexpressed in both 1-2 mm *Fas1-2* ears and 2-3 mm *Fas1-R* ears. The expression level of *drl2* was 2-fold higher in *Fas1-2* compared to normal siblings in samples containing 1-2 mm ears surrounded by immature leaf primordia (Fig. 4A, 4C). When all leaf tissues were dissected away from 2-3 mm *Fas1-R* ears, the elevated expression level of *drl2* was more obvious (Fig. 4B, 4D). Neither *zmm8* nor *drl2* were expressed in the 2-3 mm immature ears of *Fas1-Rev1*, *Fas1-Rev2*, B97 or Oh43 (Fig. 4B, and *SI Appendix*, Fig. S3F-G). Both genes were expressed in *Fas1-Rev1* and *Fas1-Rev2* at later ear developmental stages (5-8 mm and 8-12 mm) which contain FMs and floral organs (*SI Appendix*, Fig. S3F-G).

In order to explore the possibility of different transcripts originating within the Fas1 locus, we carried out 5'-RACE of zmm8 and drl2 to amplify all possible transcripts in immature ears of Fas1-R/+ (A188 background) and A188. After amplification with gene specific primers (GSP1 and GSP2) and sub-cloning, more than 20 clones were sequenced. Three types of zmm8 full-length cDNA have the same coding sequence but different 5'untranslated region (UTR) in Fas1-R/+ (Fig. 4E). Genomic DNA amplifications with primers designed specifically for the novel Fas1-R 5'-UTR showed zmm8-type2 and zmm8-type3 fragments existed in Fas1-R/+ only and not in A188 genomic DNA (Fig. 4G). When evaluating B73, B97 and Oh43, we found zmm8-type3 sequence to be unique to the Fas1 alleles (Fas1-R, Fas1-Rev1 and Fas1-Rev2) (Fig. 4E, 4G, and SI Appendix, Fig. S3A-C). drl2-specific primers revealed two types of 5'-UTR sequences in Fas1-R/+, one in common with A188 and likely arising from the wild-type copy in the heterozygote. The other product had several indels and insertions located 1 to -250 bp upstream of the ATG (Fig. 4F). The novel sequence in Fas1-R was also confirmed by gDNA amplifications. The drl2-type1 was present in other inbreds, but drl2-type2 was found only in the Fas1-Rrelated alleles (Fas1-R, Fas1-Rev1 and Fas1-Rev2) (Fig. 4G, and SI Appendix, Fig. S3D-E).

219

220221

222

223

224

225

226

227

228

229

230231

232233

234

235

236

237

238

239

240

241

242

243

244

245

246

247

248

249

250

251

252

253

254255

256257

Although the *Fas1* revertants contain the *Fas1* unique 5' UTR genomic sequence for *zmm8* and *drl2*, these sequences are not expressed. Sequencing of the transcripts showed they were zmm8-type2 and drl2-type1. These findings suggest that it is not simply additional gene copies that lead to the early misexpression of these two transcription factors, and thus, the *Fas1* phenotype, but novel promoters or enhancers resulting from the gene rearrangements unique to *Fas1-2* and *Fas1-R*.

To understand how misexpression of zmm8 and drl2 leads to a fascicled inflorescence phenotype, we carried out *in situ* hybridization using antisense probes. *zmm8* is expressed only in the upper floret and not in the lower floret of each spikelet (26). drl2 is expressed in leaf primordia of the shoot apical meristem (SAM) and lateral floral primordia of the floret, controlling midrib patterning and FM determinacy (27,28). Consistent with previous reports (26), we did not detect zmm8 expression in the earlier stage of normal ear development when SPMs are initiating, but identified zmm8 expression in FM primordia (Fig. 4H #1-#2). Intriguingly, in Fas1-2 ears, zmm8 signal was observed in the IMs and SPMs (Fig. 4H #3-#5), although it was not observed in the sunken domain of the inflorescence tip (Fig. 4H #4). In normal ears, drl2 mRNA was not visible in 1 mm ears (Fig. 4H #6), but was detected in lateral floral primordia of later stages (Fig. 4H #7). In the Fas1-2 ears, however, drl2 signals could be observed in the ectopic IMs and SPMs (Fig. 4H #8-#10). These results show that zmm8 and drl2 are misexpressed in the IMs of the Fas1 ear, which may suppress the meristematic activities of the central region and promote meristematic activities of the peripheral region, leading to highly branched "bundled" inflorescences.

In order to determine if simple overexpression of *zmm8* could create the *Fas1* phenotype, we overexpressed the gene behind the *ubiquitin* promoter in the inbred line ZZC01. The plants had a normal IM, although the expression levels were much higher than controls (*SI Appendix*, Fig. S4*A*-4*B*). We also knocked out *zmm8* and its paralog *zmm14* using CRISPR/Cas9. The loss of function phenotype is reminiscent of the triple mutant of *drl1*, *drl2* and the maize AGAMOUS ortholog, *zag1* (28). The FM shows failure of floral organ conversion and instead forms indeterminate branches with increased and elongated glumes (*SI Appendix*, Fig. S4*H*-4*L*). This result suggests that *zmm8/14* and *drl1/2* have the capacity to regulate similar floral developmental pathways. To test the possibility that ZMM8 and DRL2 interact with each other to cause the *Fas1* phenotype, we carried out yeast two hybrid and luciferase complementation image assays. We found that ZMM8 physically interacted with DRL2 in yeast and in tobacco (*SI Appendix*, Fig. S4*F*-4*G*). Given that the normal expression patterns of *drl2* and *zmm8* do not overlap (Fig. 4H), it is possible that the misexpression of both *zmm8* and *drl2* in overlapping domains in *Fas1* mutants allows for an interaction that does not occur when only *zmm8* is misexpressed.

Based on the gene copy number variations and the misexpression pattern, we hypothesize that the extra copies led to the formation of novel promoters or enhancers, which result in spatial and temporal misexpression of both *zmm8* and *drl2* in *Fas1* IMs. One of the revertants, *Fas1-Rev1*, maintains the *Fas1-R* genomic structure, but expresses zmm8-type2 and drl2-type1 transcripts with an additional truncated *drl2*, which could be the possible reason for the phenotype reversion. The other revertant, *Fas1-Rev2*, lost an extra copy of *zmm8*, expresses zmm8-type2, and drl2-type1. Neither revertant expresses the *Fas1-R* specific transcripts (zmm8-type3 and drl2-type2), and the transcripts they do express only accumulate at the later floral development stage (Fig. 4*G*, and *SI Appendix*, Fig. S3*F-G*). We propose that the novel promoter(s) containing zmm8-type3 and/or drl2-type2 related sequences are required for the misexpression of *zmm8* and *drl2* in *Fas1-R*.

Central/peripheral zone markers are misexpressed in Fas1 inflorescence meristems

To better understand the biological processes that are altered in Fas1, 1-2 mm immature ears containing adjacent immature leaf primordia of Fas1-2 and normal siblings were collected for RNA sequencing. In total, we detected 3227 up-regulation and 2284 down-regulation genes (q < 0.05) (Fig. 5A). We found that zmm8 was not expressed in wild type but was expressed at a low level (0.35 fragments per kilo base per million on an average) in Fas1-2, the expression of dr12 was three-fold higher in Fas1-2 (SIAppendix, Fig. S5A).

We focused on expression of genes related with organ polarity and inflorescence architecture and found meristem marker genes, such as *knotted1* (*kn1*), *wuschel1* (*wus1*) and *wus2*, were dramatically down regulated in *Fas1-2*. Several other genes which are specifically expressed in the shoot apical meristem tip, including maize orthologs of *DRP4A*, *LOG7*, *AGO18A*, *OC564*, *OC340* (29) were also down regulated significantly (Fig.

5B, and SI Appendix, Table S4). Given that YABBY genes play a role in polarity in 297 Arabidopsis, we examined other polarity markers: adaxial/central zone identity genes 298 299 PHABULOSA (PHB),PHAVOLUTA (PHV), and REVOLUTA abaxial/peripheral zone promoting genes YABBY2 and YABBY3, KANADI1, KANADI2, 300 KANADI3. The PHB (ath14) maize homologues phb061, phb489, phb699 and phb246, are 301 all down regulated in Fas1-2; while the AS2 homologous genes (lob27 and lob31), and 302 KANADI homologous genes (kanadi1, kanadi3, kanadi-like, Zmglk1, mwp1) are all up 303 regulated in Fas1-2. Intriguingly, 12/13 of the differentially expressed YABBYs (including 304 Arabidopsis YABBY2, YABBY3 and YABBY5 homologous genes) were also up-regulated in 305 Fas1-2 (Fig. 5B, and SI Appendix, Table S4). Down-regulation of central zone genes and 306 307 up-regulation of peripheral zone genes suggest that cell fate and organ polarity of Fas1-2 IMs are altered. 308

309

310 311

312

313

314

315

316

317

318

319

320

321

322

323

324 325

326

327328

329

330

331

332333

334335

Expression levels of these genes were also analyzed in Fas1-R (A188) with 2-3 mm ears using qRT-PCR. The data revealed that markers for meristematic activity and central zone showed similar expression pattern to that in Fas1-2. In contrast, markers for peripheral promoting genes (lob27, kanadi1, Zmglk1, mwp1, yabby9/10/14/15) had reduced expression, showing the opposite trends with that in Fas1-2 (SI Appendix, Fig S3C). These differences could be attributed from differences in ear developmental stage (30), inbred background, or allele.

To further explore the cell fate changes in Fas1, five differentially expressed marker genes were selected for in situ hybridization. We found the meristem marker knotted1, strongly expressed in the normal ear, covering the entire region of the IM (Fig. 5C # 1). In Fas1-2 with two ectopic IM, the expression domain was reduced (Fig. 5C #2). The transcripts of phb489, homologous to PHAB, are highly enriched in the central region of the tip of a normal ear, and are also detected in the boundary region between the IM and SPM primordia (Fig. 5C #3). In Fas1-2, which has two independent growth axes, no phb489 signal was detected in the central region of this stage and only a weak signal in the peripheral region (Fig.5C #7-#8). oc616 has been reported as specifically expressed in the center of the SAM (29). We found the transcript signal distributed throughout the immature ear in B73 (Fig. 5C #6), but it was strong in the apical cells and very weak in the central region of Fas1-2 IM with two bifurcations (Fig. 5C #9-#10). The repressed expression of these two central zone marker genes suggests that growth of the central region in the Fas1 ear has been suppressed. lob27, the as2 homologous gene, is expressed in the apical meristem of B73 ear (Fig.5C #5). In Fas1-2, it is expressed in the boundary region between peripheral and center when the ear width increased (Fig. 5C #11), then shows broad expression in the ear with increased mild bifurcations, and finally appeared only in the ectopic IM (Fig. 5C # 12-#13). yabby15 (zyb15) is a robust marker of lateral organs and is absent from meristems (31–34). We found zyb15 mRNAs accumulate in the bracts and the adaxial side of the young leaf in B73 ear (Fig. 5C #6) as noted previously (31), however, in Fas1-2, it is stronger in the adaxial side of the lateral organs, and also expressed in the apical cells of the IM with two bifurcations and the bracts (Fig.5C #14-#15). In summary, these marker genes accumulate in the peripheral region of ectopic IMs but weakly in the central domain of the Fas1 ear, a pattern consistent with zmm8 and drl2. These results suggest the misexpression of zmm8 and drl2 changes central/peripheral cell fate in Fas1 IMs by targeting these genes directly or indirectly.

Discussion

The two *Fas1* alleles arose spontaneously with no available progenitors. In independent experiments, the alleles mapped to the same interval of chromosome 9, containing two genes that encode transcription factors, a MADS-box, *zmm8* and a YABBY gene, *drl2* (Fig. 3A). Both *zmm8* and *drl2* are normally expressed in floral organs, with *zmm8* in the FM itself and *drl2* in the lateral organs of the FM (Fig. 4H #1-#2, #6-#7). RNA analysis shows that in the *Fas1* mutants, expression of both genes is increased and shifted earlier in development (Fig. 4 A-C). *In situ* hybridization in *Fas1* shows expression in the IM rather than the floral organs (Fig. 4.H #3-#5, #8-#10). DNA blots show extra copies of both genes in the *Fas1* alleles (Fig. 3C). Given that the inbred B97 also has a duplication of this locus, but both *zmm8* and *drl2* maintain normal expression (*SI Appendix*, Fig. S2A-B, 3F and 3G), we hypothesize there is a novel promoter or regulatory sequence that is responsible for the misexpression. Our RNA sequencing data suggest that the misexpression of the central/peripheral genes leads to the fascicled ear and tassel with deep branching (Fig. 5).

The biological function and co-regulation of zmm8 and drl2

MADS-box genes have been classified into "ABCDE" clades, which are widely used as a framework in shaping floral organ identity (35-37). In maize, zmm8 and its duplicate, zmm14, are AGAMOUS-LIKE6 E class genes. In angiosperms, E class proteins are necessary components of B and C class tetramers (38,39). The E class SEPALLATA (1-4) genes of Arabidopsis function redundantly and in combination with A, B, C class genes. Loss-of-function mutants lose determinacy of floral meristems and display homeotic conversions (40,41). A mutant phenotype has been identified for the *zmm8* ortholog in rice, leafy hull sterile1 (lsh1) encoding OsMADS1. Missense mutations in the MADS domain of lhs1 result in open flowers with leafy lemma, palea and lodicule, reduced stamens and additional carpels. Another rice mutant in the SEPALLATA subfamily is panicle phytomer2 (carrying a mutation in OsMADS34), which converts some spikelets to branches and the flowers have elongated rudimentary glumes and sterile lemmas (42). These phenotypes suggest a function in specifying floral organ identity (43,44). Indeed, we discovered that the double mutant of zmm8/zmm14 fails to initiate floral organs and is indeterminate (SI Appendix, Fig. S4). Thus, their expression in the FM is required to promote floral organ initiation and determinacy.

YABBY proteins function to promote laminar growth of lateral organs, thus distinguishing them from the radially symmetrical SAM (33). Four of six Arabidopsis YABBY genes including FILAMENTOUS FLOWER (FIL), YABBY2, YABBY3, YABBY5 are expressed in the abaxial side of lateral organs and are responsible for abaxial cell fate identity. Loss of function of fil and yabby3 leads to narrow leaves with loss of laminar expansion (10,11). In rice, mutation of the FIL-clade gene, TONGARI-BOUSHII (TOB1), results in a prematurely terminated spikelet meristem and reduced growth of the lemma or palea in the floret (45), while the drooping leaf (dl) mutant in the CRC/DL-clade, showed a homeotic transformation of carpels into stamens and lack of midrib (46,47). In maize, drooping leaf1 (drl1) and drl2 mutants have unfused carpels in the female florets, and extra stamens in the male florets (28) in addition to the loss of midrib (27). When combined with the loss of function of maize AGAMOUS (zag1) (28), the floral meristems are more indeterminate, similar to those of zmm8/zmm14 (SI Appendix, Figure S4C). Thus, both zmm8 and drl2 affect a common process when expressed in their normal domain.

While the knockout mutant (*zmm8/zmm14*-KO) may not help solve the question of how misexpression of *zmm8* in *Fas1* leads to the fascicled phenotype, it does provide insight into the potential regulation or interaction between *zmm8* and *drl2* in *Fas1*. A gene regulatory network analysis in maize suggested that *drl1/2* and MADS-box genes, including *zmm8* and *zmm14*, are co-regulated and co-expressed (28). Indeed, we found that ZMM8 and DRL2 physically interact with each other in heterologous systems (*SI Appendix*, Fig. S4F-4G). Given the fact that overexpressing *zmm8* does not cause a *Fas1* phenotype (*SI Appendix*, Fig. S4A), our results suggest that an interaction of ZMM8 and DRL2 proteins might produce the *Fas1* phenotype, rather than it being due simply to an increase in the level of only *zmm8*. In Arabidopsis, ectopic expression of *FIL* or *YABBY3* are sufficient to specify abaxial cell fate, and high levels lead to enlarged meristems that arrest (10,11). Although it is still possible that overexpression of *drl2* alone causes the *Fas1* phenotype, *Fas1*-Rev2 lost an extra copy of *zmm8* but not *drl2*.

In summary, both *zmm8* and *drl2* have roles in regulating FM determinacy, but are not expressed in overlapping domains. In *Fas1*, the misexpression of *zmm8* and *drl2* overlaps in the immature IM, affecting cell fate in the central/peripheral zone and thereby activating an ectopic laminar program and disrupting signaling necessary for maintenance of radially symmetrical inflorescence meristems.

Tandem duplications that cause dominant phenotypes

A high reversion rate, as noted with Fas1-R, is also seen with one of the dominant alleles of Kn1, Kn1-O (48). The tandem duplication of 17 kb produced two promoters in Kn1-O, one with sequence similarity to wild type and the other in a novel position, juxtaposed to the 3'-end of the duplicated copy. The novel promoter is considered the cause of the mutant phenotype because transposon insertions into the novel promoter repressed the mutant phenotype (49). The co-dominant Tunicate locus which confers the pod corn phenotype,

in which each kernel is surrounded by derepressed glumes, palea and lemma, is a duplication of another MADS-box gene, *zmm19* (50–52), and the ectopic expression pattern of *zmm19* was caused by the rearrangement of a 5'-regulatory region of *zmm19* by an unknown mechanism.

We hypothesize that a similar event occurred at Fas1; novel regulatory sequences that initiate expression of both zmm8 and drl2 earlier than normal cause the phenotype. Given the Fas1-R specific 5'-UTR for both zmm8 and drl2, sequence variation may extend to the longer upstream region of the duplicated genes to produce novel promoters or regulatory regions. In fact, this region may harbor the variation in Fas1-Rev1, which is normal in phenotype yet retains the copy number variation of Fas1-R. Although there are duplicated copies of zmm8 and or drl2 in inbreds B97 and Oh43, the Fas1 mutants have additional copies, the Fas1-R specific 5'-UTRs of zmm8 and drl2 are not present in B97 and Oh43, and misexpression of zmm8 and drl2 is not detected at the ear transition stage in these inbreds. We hypothesize that in Fas1 alleles, novel promoters or enhancers formed as a result of the duplication events. Distal regulation of gene expression has been described for teosinte branched1 (53) and unbranched3 (54). The unknown regulatory sequences at Fas1, whether they are enhancer-promoter or promoter-promoter chromatin interactions, cause ectopic expression of zmm8 and drl2 at an earlier stage than in wild type. Finding the exact sequence of these promoters will require further study, but could be used for reengineering gene expression to improve maize ear architecture.

Establishment of radial symmetry of the maize inflorescence meristem

The maize IM is radially symmetrical, containing a central/peripheral axis (55). Gene expression patterns and mutant phenotypes connect the central/peripheral axis of symmetric organs to the adaxial/abaxial axis of laminar lateral organs (2,8). The ectopic expression of *drl2* and *zmm8* was accompanied by the up-regulation of peripheral cell fate promoting genes like *LOBs*, *KANADIs* and *YABBYs*, which may promote the meristematic activity of the peripheral cells in the IM. The meristem-activating genes *kn1*, *wus*, *OCs*, and central zone marker genes *PHB* are downregulated in the apical meristem of the *Fas1* ear, showing suppression of the meristem central zone (Fig. 5*D-E*).

A similar phenotype of bifurcated inflorescence meristems has been described in rice for the double mutant of the TOPLESS (TPL)-like transcriptional corepressor encoding gene aberrant spikelet and panicle1 (asp1) and Arabidopsis CLV3 homolog floral organ number2 (fon2) (56). Similar to Fas1, the IM was enlarged and then bifurcated. The asp1;fon2 phenotype differs in that the bifurcated IMs retain radial symmetry. Interestingly, loss of the WUS ortholog, tillers absent1 (tab1) did not affect this phenotype (56). It would be interesting to know if YABBY genes are differentially expressed in this mutant. If not, it appears there is more than one mechanism to bifurcate the IM.

Although mutants in maize orthologs of the *CLV* genes have enlarged meristems similar to those of Fas1, we do not think these genes are central to this phenotype. The CLV2 ortholog, fasciated ear2 and fon2-like cle protein1 are down regulated in Fas1-2. The mutants of these genes have loss of function phenotypes that cause fasciation by loss of spatial regulation of wus. However, both wus 1 and wus 2 were also down-regulated in Fas 1-2. Other genes in the CLV-WUS pathway such as Wuschel Homeobox (WOX) genes, Clavata (clv3)/ embryo surrounding region (ESR) (CLE) genes, G protein encoding genes, and Barely any meristem genes were not consistently differentially expressed (SI Appendix, Fig S5B). We hypothesize that rather than differential expression of genes in the CLV-WUS pathway, the Fas1 phenotype is due to differential expression of genes specifying central/peripheral zone cell fate which then activates a laminar program and disrupts maintenance of a radially symmetrical inflorescence meristem. We propose that the duplications and rearrangements of zmm8 and drl2 in Fas1 alleles cause their misexpression in the IM at the transition stage, leading to suppression of meristematic activity of central cells and promotion of meristematic activity of peripheral cells, resulting in the repeatedly bifurcated inflorescences of this neomorphic mutant.

468469 Materials and Methods

Plant materials and phenotypic characterization

The dominant Fascicled ear1-Reference allele, (Fas1-R), was obtained from the Maize Cooperative Center and was backcrossed to B73 nine times and to A188 six times. Phenotypic characterization was done in backcross progenies and F_2 families. Paul Weatherwax first described the Fas1 mutant in 1954 (25), contrary to erroneous citations of an earlier description. Based on sequence similarity to B97, we purport that this allele is the "recent" allele described by Paul Weatherwax (23). Fas1-Rev1 and Fas1-Rev2 were isolated in two revertant screens with 1/1878 and 1/1500 revertants per total, respectively. Fas1-R (Orr) was a gift from Marshall Sundberg after it had been maintained by Alan Orr, in the original landrace in which it was found. This line was the progenitor for Fas1-Rev1. Fas1-2 came from a Chinese breeding line. It was crossed to B73 then self-pollinated to construct F_2 populations, and backcrossed to B73 for observations. Fas1-2/B73 F_1 individuals appear similar to Fas1-2 homozygous mutants with bifurcated inflorescences. In the F_2 populations with 282 individuals, there were 207 mutants and 75 wild type plants, consistent with the expected ratio of 3:1 (Chi-square test, P < 0.001). Inflorescence traits were measured for both alleles (SI Appendix, Table S1-S2).

For the *zmm8* overexpression line, the *zmm8* coding sequence was cloned into the modified *pCAMBIA3301* vector to create the recombinant vector *pUbi::zmm8+YFP*. For the *zmm8/14* CRISPR-Cas9 knockout line, we designed two gRNAs for each gene and ligated four gRNAs into vector *CPB-ZmUbi-hspCas* to produce recombinant vector *ZmpU6::zmm8* (*gRNA1*) + *OspU3::zmm8* (*gRNA2*)+*ZmpU6::zmm14*

- 492 (gRNA1)+OspU3::zmm14 (gRNA2). gRNA sequences list in SI Appendix, Table S3. All
- 493 genetic transformation was performed by the China National Seed Group Corp (Wuhan)
- in the transgenic genetic background is ZZC01. Phenotypic characterization was done on
- 495 T0 plants. For the zmm8 overexpression line, two independent transgenic events of five
- and eight transgenic plants each were observed; and for the zmm8/14 CRISPR-Cas9
- 497 knockout line, three independent events with three editing types for each gene were
- 498 detected (SI Appendix, Table S5).

Scanning electron microscopy observation

- Immature ear and tassel from 1 to 5 mm of the Fas1-2 (in B73), Fas1-R (in A188)
- 501 homozygotes or heterozygotes and wild-type siblings (in B73) were collected and fixed in
- 502 50% FAA solution (50% ethanol, 3.7% formaldehyde and 5% glacial acetic acid (V/V/V)),
- then dehydrated through a graded series of ethanol from 30 to 95%. Tissue were dried using
- a Tousimis autosamdri-815 critical point dryer, sputter coated with gold palladium for 30-
- 505 60s, and observed using a Jeol JSM-7900F scanning electron microscope as previously
- 506 described (57).

499

507 508

Fine mapping of Fas1 locus

- 509 Fas1-R was first mapped between visible markers wx1 and Rld, on the long arm of
- 510 chromosome 9 using waxy translocation lines (24). In addition, Fas1-R was fine-mapped
- 511 in 426 backcrossing individuals (A188 as recurrent parent) with molecular markers
- developed from the syntenic region of B73 using the IBM2 2005 Neighbors genetic map
- available at MaizeGDB (58). Primers used in the study are listed in (SI Appendix, Table
- 514 S3).

524

- For the Fas1-2 mapping, 286 F₂ individuals derived from Fas1-2×B73 was constructed.
- For the Bulked-Segregant RNA sequencing mapping, 30/30 1-2 cm ears of the Fas1-2 and
- 517 wild-type individuals were collected for RNA extraction (with Trizol reagent (Life
- 518 Technologies, Carlsbad, CA, USA)). The two RNA library were sequenced on a NextSeq
- 519 441 Illumina platform with PE75 (paired-end), and 18 Gb data were aligned to the maize
- 520 genome B73 RefGen V3 (AGPv3.31) using Tophat2-PE (2.0.9) (59). Then, the initial
- mapping region was narrowed to ~9 Mb, flanked by markers *umc2159* and *phi108411*.
- Furthermore, to fine map the Fas1-2, 15 markers were developed (SI Appendix, Table S3),
- and a large mapping population with 7680 F₂ individuals was constructed.

DNA Blotting

- Approximately 1.5g of B73 leaf tissue, wildtype, Fas1-2, Fas1-R, Fas1-Rev1 and Fas-
- 526 Rev2 were used for high quality (>1μg/μl) genomic DNA extraction by
- hexadecyltrimethylammonium bromide (CTAB) methods. Approximately 30µg DNA
- sample was separately digested by restriction enzyme *Hind*III (50 U with 10×M buffer),
- 529 XbaI (50 U with 10×M buffer) and NcoI (50 U with 10×K buffer), 37°C, 16h. The digested

- 530 gDNA products were separated by electrophoresis at 30 V for 16 h on 0.8% agarose gel
- with 1×TAE buffer (40 mM Tris base, 20 mM acetic acid, 1 mM EDTA disodium salt
- dehydrate, PH 8.3), then transferred to a positively charged nylon membrane using a
- capillary method. Both zmm8 and drl2 gene specific probes (SI Appendix, Table S3) were
- labeled by Digoxin, then blotted and detected using Roche southern blot kit (DIG High
- 535 Prime DNA Labeling and Detection Starter Kit II, Roche).

Gene expression analysis

536

548

561

- To analyze the expression pattern of zmm8 and drl2, twenty to thirty 1-2 mm length
- immature ears of the Fas1-2 (B73) and wild type (B73), six to eight 2-3 mm length ears of
- the Fas1-R (A188) and wild type (A188) were collected, respectively. Total RNA was
- 540 extracted using TRIzol reagent (Life Technologies) according to the manufacturer's
- 541 instructions, purified, and reverse-transcribed using an EasyScript One-step gDNA-
- removal and cDNA-Synthesis Supermix Kit (Transgene, Beijing, China). Gene-specific
- primers (SI Appendix, Table S3) combining 2×GoTaq Green Master Mix (Promega,
- Madison, USA) or SYBR Green PCR Master Mix (KAPA, Beijing, China) were used for
- RT-PCR and qPCR, respectively. qPCR was performed with three biological and three
- 546 technical replicates, maize beta-actin (NM 001155179) gene was used as an internal
- 547 control. RT-PCR and RNA sequencing were performed with three biological replicates.

Rapid-amplification of cDNA ends (RACE)

- Gene 5'-RACE was performed with RNA extracted from 2-3 mm length ears of Fas1-R
- 550 heterozygotes (A188), wild type (A188), Fas1-2 homozygotes, and 5-8 mm length ears of
- 551 Fas1-Rev1, Fas1-Rev2 heterozygotes, and A188, B73 using GeneRacer Kit (Invitrogen,
- L1502-02). After PCR amplification with GeneRacer 5 primer and reverse GSP1 (gene-
- specific primer1) using 2×GoTaq Green Master Mix (Promega, Madison, USA), then
- followed by the second cycle PCR amplification with GeneRacer 5 primer and reverse
- 555 GSP2. The PCR products were purified using OIAquick PCR purification kit (Oiagen,
- 556 Germany), the purified PCR products were cloned into pGEM-Teasy vector (Promega,
- Madison, USA). At least 20 positive clones were sequenced for each sample. The
- sequences were analyzed using CLC sequence viewer 7.6, gene models of zmm8 and drl2
- in B73 RefGen v4were used to guide annotation. Gene-specific primers for RACE assay
- were listed in (SI Appendix, Table S3).

Transcriptome profiling

- Approximately 1-2 mm length immature ears of the Fas1-2 (B73) and wild type (B73)
- were collected for RNA extraction. After purification, RNAs were used for RNA
- sequencing by Beijing Genomics Institute (BGI, Shenzhen, China) on the Illumina system
- 565 HiSeq2500 (Illumina Inc., San Diego, CA, USA). The FASTX-Toolkit was used to
- preprocessed raw reads (60), followed by FASTQC program to assess the clean reads (61),

- then aligned to the B73 RefGen v4using TOPHAT v.2.1.0 (59). CUFFLINKS v.2.1.1 (62)
- was used to normalize and estimate the gene expression level based on fragments per
- kilobase of transcript per million reads (63). The differentially expressed genes (DEGs)
- were also calculated by CUFFLINKS v.2.1.1 at a significance level of p < 0.05. The DEGs
- were listed in (SI Appendix, Table S3).

mRNA in situ hybridization

- 573 1-5 mm length immature ears of Fas1-2 (B73) and B73 were harvested and fixed in 4%
- 574 PFA solution (4g of paraformaldehyde (Sigma-Aldrich) dissolved in 100 mL of 1× PBS
- 575 (10mM Na₂HPO₄, 1.8mM KH₂PO₄, 0.137M NaCl, 2.7mM KCl, pH 7.4), pH 6.5 7), then
- dehydrated with an ethanol series and embedded in Paraplast Plus (Sigma, 513 St. Louis,
- MO, USA), and sectioned to a thickness of 8 μm. Anti-sense RNA probes were amplified
- with gene specific primers (SI Appendix, Table S3) adding an SP6 sequence, then purified
- and synthesized using SP6 RNA polymerase with digoxigenin-UTP as a label (Roche),
- respectively. RNA hybridization and immunologic detection were performed as described
- 581 previously (64).

572

582

597 598

Protein-protein interactions

- To analysis protein-protein interactions, firefly luciferase complementation imaging (LCI)
- and yeast one-hybrid assays (Y2H) were performed. In LCI, the full-length CDS of zmm8
- and *drl2* were cloned into JW771 (NLUC) and JW772 (CLUC) to produce ZMM8–NLUC
- and DRL2-CLUC vectors, respectively. Agrobacterium tumefaciens GV3101 cells were
- 587 used for transformation, and the *Nicotiana benthamiana* was used for transient expression
- with three replicates. After 48 h of growth under a 16 h-light/8 h-dark cycle, 1 mM luciferin
- 589 (Promega) was applied to the abaxial epidermis of each leaf, and the luciferin signal were
- 590 detected and captured as described in (54).
- For Y2H, the full-length CDS of *zmm8* and *drl2* were cloned into pGBKT7 and pGADT7
- 592 (Clontech, CA, USA) to generate p GBKT7–ZMM8 and pGADT7–DRL2, respectively.
- The constructs were transformed into yeast strain AH109 as described in (65), and Yeast
- 594 two hybrid assays were performed according to the description of Matchmaker Gold Two-
- 595 Hybrid System user manual (66). Primers used for vector constructions were listed in (SI
- 596 Appendix, Table S3).

Acknowledgments

- We thank Joshua Strable, Sam Leiboff, Zhaobin Dong, and Lei Liu for reviewing the
- 600 manuscript; Zengdong Tan and Manfei Li for the RNA sequencing analysis, Katarina
- Makmuri for assistance with mapping Fas1-R, Margaret Woodhouse of MaizeGDB for
- assistance with the NAM genomes and George Chuck and Nathalie Bolduc for technical
- advice. We also thank De Wood for assistance with scanning electron microscopy at the
- 604 USDA, Albany, CA. This work was supported by the National Natural Science Foundation
- of China (91935305), the National Key Research and Development Program of China

(2016YFD0100404), and the US National Science Foundation (IOS-1733606).

608 References

- Turnbull, C. G. Plant architecture and its manipulation. Blackwell Publishing. (2005).
- Engstrom, E. M., Izhaki, A. & Bowman, J. L. Promoter Bashing, microRNAs, and Knox Genes. New Insights, Regulators, and Targets-of-Regulation in the Establishment of Lateral Organ Polarity in Arabidopsis. *Plant Physiol.* **135**, 685–694 (2004).
- Wardlaw, C. W. Experimental investigation of leaf formation, symmetry and orientation in ferns. *Nature*. doi:10.1038/175115a0 (1955).
- 517 4. Sussex, I. M. Morphogenesis in Solanum tuberosum L.: experimental investigation of lea dorsiventrality and orientation in the juvenile shoot. *Phytomorphology* (1955).
- 5. SNOW, M. & SNOW, R. THE DORSIVENTRALITY OF LEAF PRIMORDIA. *New Phytol.* doi:10.1111/j.1469-8137.1959.tb05351.x. (1959).
- 621 6. Waites, R. & Hudson, A. *phantastica*: A gene required for dorsoventrality of leaves in Antirrhinum majus. *Development.* **121**, 2143-2154 (1995).
- 7. Yamaguchi, T., Nukazuka, A., & Tsukaya, H. Leaf adaxial—abaxial polarity specification and lamina outgrowth: evolution and development. *Plant and Cell Physiology*. **53**, 1180-1194 (2012).
- 626 8. Caggiano, M.P. *et al.* Cell type boundaries organize plant development. *Elife.* **6**, 1–627 32 (2017).
- 628 9. Golz, J. F., Roccaro, M., Kuzoff, R. & Hudson, A. *GRAMINIFOLIA* promotes growth and polarity of Antirrhinum leaves. *Development*. doi:10.1242/dev.01221 (2004).
- 631 10. Sawa, S. *et al. FILAMENTOUS FLOWER*, a meristem and organ identity gene of Arabidopsis, encodes a protein with a zinc finger and HMG-related domains. *Genes Dev.* **13**, 1079–1088 (1999).
- 634 11. Siegfried, K. R. *et al.* Members of the YABBY gene family specify abaxial cell fate in Arabidopsis. *Development.* **126**, 4117–4128 (1999).
- 636 12. Chitwood, D. H., Guo, M., Nogueira, F. T. S., Timmermans, M. C. P. Establishing leaf polarity: The role of small RNAs and positional signals in the shoot apex.

 638 Development. 134, 13–23 (2007).
- Husbands, A. Y., Chitwood, D. H., Plavskin, Y. & Timmermans, M. C. P. Signals and prepatterns: New insights into organ polarity in plants. *Genes and Development*. doi:10.1101/gad.1819909 (2009).
- Howman, J. L., Eshed, Y., & Baum, S. F. Establishment of polarity in angiosperm lateral organs. *TRENDS in Genetic.* **18**, 134-141 (2002).
- Daum, G., Medzihradszky, A., Suzaki, T. & Lohmann, J. U. A mechanistic framework for noncell autonomous stem cell induction in Arabidopsis. *Proc. Natl. Acad. Sci. U. S. A.* doi:10.1073/pnas.1406446111 (2014).
- 647 16. Somssich, M., Je, B. Il, Simon, R. & Jackson, D. CLAVATA-WUSCHEL signaling in the shoot meristem. *Development.* **143**, 3238-3248 (2016).

- 549 17. Je, B. Il *et al.* The CLAVATA receptor *FASCIATED EAR2* responds to distinct CLE peptides by signaling through two downstream effectors. *eLife.* DOI:10.7554/eLife.35673 (2018).
- 652 18. Bommert, P. *et al.* thick tassel dwarf1 encodes a putative maize ortholog of the Arabidopsis *CLAVATA1* leucine-rich repeat receptor-like kinase. *Development.* **132**, 1235–1245 (2005).
- Taguchi-Shiobara, F., Yuan, Z., Hake, S. & Jackson, D. The *fasciated ear2* gene encodes a leucine-rich repeat receptor-like protein that regulates shoot meristem proliferation in maize. *Genes Dev.* **15**, 2755–2766 (2001).
- 558 20. Je, B. Il *et al.* Signaling from maize organ primordia via *FASCIATED EAR3* regulates stem cell proliferation and yield traits. *Nat. Genet.* doi:10.1038/ng.3567 (2016).
- Bonnett OT. Ear and Tassel Development in Maize. *Ann Missouri Bot Gard.* **35**, 269–87 (1948).
- Orr, A. R., Haas, G. & Sundberg, M. D. Organogenesis of Fascicled ear mutant inflorescences in maize (Poaceae). *Am. J. Bot.* doi:10.2307/2445808 (1997).
- Weatherwax, P. How the Indian Improved Corn in *Indian Corn in Old America*. 182–207 (1954).
- Laughnan, J. R. & Gabay-Laughnan, S. The Placement of Genes Using waxy-Marked Reciprocal Translocations. in *The Maize Handbook*. doi:10.1007/978-1-4612-2694-9 29 (1994).
- 670 25. Mount, D. W. Using the Basic Local Alignment Search Tool (BLAST). *Cold Spring* 671 *Harb. Protoc.* doi:10.1101/pdb.top17 (2007)
- Cacharron, J., Saedler, H. & Theissen, G. Expression of MADS box genes ZMM8
 and ZMM14 during inflorescence development of Zea mays discriminates between
 the upper and the lower floret of each spikelet. Dev. Genes Evol.
 doi:10.1007/s004270050271 (1999).
- 576 Strable, J. et al. Maize YABBY Genes drooping leaf1 and drooping leaf2 Regulate Plant Architecture. Plant Cell. 29, 1622–1641 (2017).
- 578 28. Strable, J. & Vollbrecht, E. Maize YABBY genes *drooping leaf1* and *drooping leaf2* regulate floret development and floral meristem determinacy. *Development*. doi:10.1242/dev.171181 (2019).
- Knauer, S. *et al.* A high-resolution gene expression atlas links dedicated meristem genes to key architectural traits. *Genome Res.* **29**, 1962–1973 (2019).
- 683 30. Eveland, A. L. *et al.* Regulatory modules controlling maize inflorescence architecture. *Genome Res.* **24**, 431–43 (2014).
- Juarez, M. T., Twigg, R. W. & Timmermans, M. C. P. Specification of adaxial cell fate during maize leaf. Development. **131**, 4533-4544 (2004).
- Goldshmidt, A., Alvarez, J. P., Bowman, J. L. & Eshed, Y. Signals derived from *YABBY* gene activities in organ primordia regulate growth and partitioning of Arabidopsis shoot apical meristems. *Plant Cell*. doi:10.1105/tpc.107.057877 (2008).
- 691 33. Sarojam, R. *et al.* Differentiating Arabidopsis shoots from leaves by combined YABBY activities. *Plant Cell.* doi:10.1105/tpc.110.075853 (2010).

- 693 34. Whipple, C. J. *et al.* A conserved mechanism of bract suppression in the grass family. *Plant Cell.* **22**, 565–578 (2010).
- 695 35. Bartlett, M. E. *et al.* The Maize PI/GLO Ortholog Zmm16/sterile tassel *silky ear1* Interacts with the Zygomorphy and Sex Determination Pathways in Flower Development. *Plant Cell.* **27**, 3081–3098 (2015).
- 698 36. Bowman, J. L., Smyth, D. R. & Meyerowitz, E. M. The ABC model of flower development: then and now. **139**, 4095–4098 (2012).
- 700 37. Callens, C., Tucker, M. R., Zhang, D. & Wilson, Z. A. Dissecting the role of MADS-701 box genes in monocot floral development and diversity. **69**, 2435–2459 (2018).
- 702 38. Theissen, G. & Saedler, H. Plant biology. Floral quartets. *Nature*. doi:10.1038/35054172 (2001).
- 704 39. Smaczniak, C. *et al.* Characterization of MADS-domain transcription factor complexes in Arabidopsis flower development. *Proc. Natl. Acad. Sci. U. S. A.*. doi:10.1073/pnas.1112871109 (2012).
- 707 40. Pelaz, S., Ditta, G. S., Baumann, E., Wisman, E. & Yanofsky, M. F. B and C floral 708 organ identity functions require SEPALLATTA MADS-box genes. *Nature*. 709 doi:10.1038/35012103 (2000).
- 710 41. Ditta, G., Pinyopich, A., Robles, P., Pelaz, S. & Yanofsky, M. F. The *SEP4* gene of Arabidopsis thaliana functions in floral organ and meristem identity. *Curr. Biol.* doi:10.1016/j.cub.2004.10.028 (2004).
- 713 42. Kobayashi, K., Maekawa, M., Miyao, A., Hirochika, H., Kyozuka, J. *PANICLE* 714 *PHYTOMER2 (PAP2)*, encoding a SEPALLATA subfamily MADS-box protein, 715 positively controls spikelet meristem identity in rice. *Plant Cell Physiol.* **51**, 47– 716 57(2010).
- Jeon, J. S. *et al. leafy hull sterile 1* is a homeotic mutation in a rice MADS box gene affecting rice flower development. *Plant Cell.* doi:10.1105/tpc.12.6.871 (2000).
- Prasad, K., Parameswaran, S. & Vijayraghavan, U. *OsMADS1*, a rice MADS-box factor, controls differentiation of specific cell types in the lemma and palea and is an early-acting regulator of inner floral organs. *Plant J.* doi:10.1111/j.1365-313X.2005.02504.x (2005).
- Tanaka, W. *et al.* The YABBY gene *TONGARI-BOUSHI1* is involved in lateral organ development and maintenance of meristem organization in the rice spikelet. *Plant Cell.* **24**, 80–95(2012).
- 726 46. Yamaguchi, T. *et al.* The YABBY Gene *DROOPING LEAF* Regulates Carpel Specification and Midrib Development in Oryza sativa. **16**, 500–509 (2004).
- 728 47. Nagasawa, N. *et al. SUPERWOMAN1* and *DROOPING LEAF* genes control floral organ identity in rice. *Development*. doi:10.1242/dev.00294 (2003).
- Wang, L. *et al.* Ectopic expression of *OsMADS1* caused dwarfism and spikelet alteration in rice. *Plant Growth Regul.* doi:10.1007/s10725-016-0220-9 (2017).
- 49. Lee, J. Y., Baum, S. F., Alvarez, J., Patel, A., Chitwood, D. H., & Bowman, J. L.
 Activation of CRABS CLAW in the Nectaries and Carpels of Arabidopsis. The
 Plant cell. 17, 25–36 (2005).
- Sieber, P., Petrascheck, M., Barberis, A. & Schneitz, K. Organ polarity in arabidopsis *NOZZLE* physically interacts with members of the YABBY family.
 Plant Physiol. doi:10.1104/pp.104.040154 (2004).

- 738 51. Theißen, G., Melzer, R. & Ruümpler, F. MADS-domain transcription factors and the floral quartet model of flower development: Linking plant development and evolution. *Development*. doi:10.1242/dev.134080 (2016).
- 52. Bartlett, M. E. Changing MADS-Box transcription factor protein-protein interactions as a mechanism for generating floral morphological diversity. in *Integrative and Comparative Biology*. doi:10.1093/icb/icx067 (2017).
- 744 48. Veit, B., Vollbrecht, E., Mathern, J. & Hake, S. A tandem duplication causes the *Kn1-O* allele of *knotted*, a dominant morphological mutant of maize. *Genetics*. **125**, 623–631 (1990).
- T47 49. Lowe, B., Mathern, J. & Hake, S. Active Mutator elements suppress the knotted phenotype and increase recombination at the *Kn1-O* tandem duplication. *Genetics*. **132**, 813-822 (1992).
- 750 50. Han, J-J., Jackson, D. & Martienssen, R. Pod Corn Is Caused by Rearrangement at the *Tunicate1 Locus. Plant Cell.* **24**, 2733–2744 (2012).
- 752 51. Wingen, L. U. *et al.* Molecular genetic basis of pod corn (Tunicate maize). *Proc.* 753 *Natl. Acad. Sci.* doi:10.1073/pnas.1111670109 (2012).
- 52. Langdale, J. A., Irish, E. E. & Nelson, T. M. Action of the Tunicate locus on maize floral development. *Dev. Genet.* doi:10.1002/dvg.1020150208 (1994).
- 756 53. Richard, M. C. *et al.* "A distant upstream enhancer at the maize domestication gene tb1 has pleiotropic effects on plant and inflorescent architecture." *Nature Genetics*. **38**, 594–597 (2006).
- 54. Du, Y., Liu, L., Peng, Y., Li, M., Zhang, Z. *Unbranched3* expression and inflorescence development is mediated by *unbranched2* and the distal enhancer, *krn4*, in maize. *PLoS Genetics*, **16**, e1008764 (2020).
- 762 55. Bonnett, OT. The Inflorescences of Maize. *Science*. 763 doi:10.1126/science.120.3107.77. (1954).
- 56. Suzuki, C., Tanaka, W., Hirano, HY. Transcriptional corepressor ASP1 and CLV-like signaling regulate meristem maintenance in rice. *Plant Physiol.* **180**, 1520–34(2019).
- Chuck, G., Whipple, C., Jackson, D. & Hake, S. The maize SBP-box transcription factor encoded by tasselsheath4 regulates bract development and the establishment of meristem boundaries. *Development.* 137, 1585–1585 (2010).
- 770 58. Portwood, J. L. *et al.* Maizegdb 2018: The maize multi-genome genetics and genomics database. *Nucleic Acids Res.* doi:10.1093/nar/gky1046 (2019).
- 772 59. Trapnell, C., Pachter, L. & Salzberg, S. L. TopHat: Discovering splice junctions with RNA-Seq. *Bioinformatics*. **25**, 1105–1111 (2009).
- 774 60. Gordon, A., Hannon, G. J. & Gordon. FASTX-Toolkit. [Online] http://hannonlab. cshl. edu/fastx_ toolkit http://hannonlab. cshl. edu/fastx_ toolkit (2014).
- 776 61. Andrews, S. FastQC. *Babraham Bioinforma*. doi:citeulike-article-id:11583827 (2010).
- 778 62. Trapnell, C. *et al.* Differential gene and transcript expression analysis of RNA-seq experiments with TopHat and Cufflinks. *Nat. Protoc.* doi:10.1038/nprot.2012.016 (2012).

- 781 63. Mortazavi, A., Williams, B. A., McCue, K., Schaeffer, L. & Wold, B. Mapping and quantifying mammalian transcriptomes by RNA-Seq. *Nat. Methods*. doi:10.1038/nmeth.1226 (2008).
- 784 64. Greb, T., Clarenz, O., Scha, E. & Schmitz, G. Molecular analysis of the *LATERAL*785 *SUPPRESSOR* gene in Arabidopsis reveals a conserved control mechanism for axillary meristem formation. *Genes & Dev.* 17, 1175-1187 (2003).
- 787 65. Takara Clontech. YEASTMAKER Yeast Transformation System 2 User Manual. System. 1, 1–15 (2001).
- 789 66. Clontech Laboratories. MatchmakerTM Gold Yeast Two-Hybrid System User 790 Manual. **092413**, 1–41(2013).

Figures and Tables 795 796

Figure 1.

794

797 798

799

800

801

802

803

804

805

806

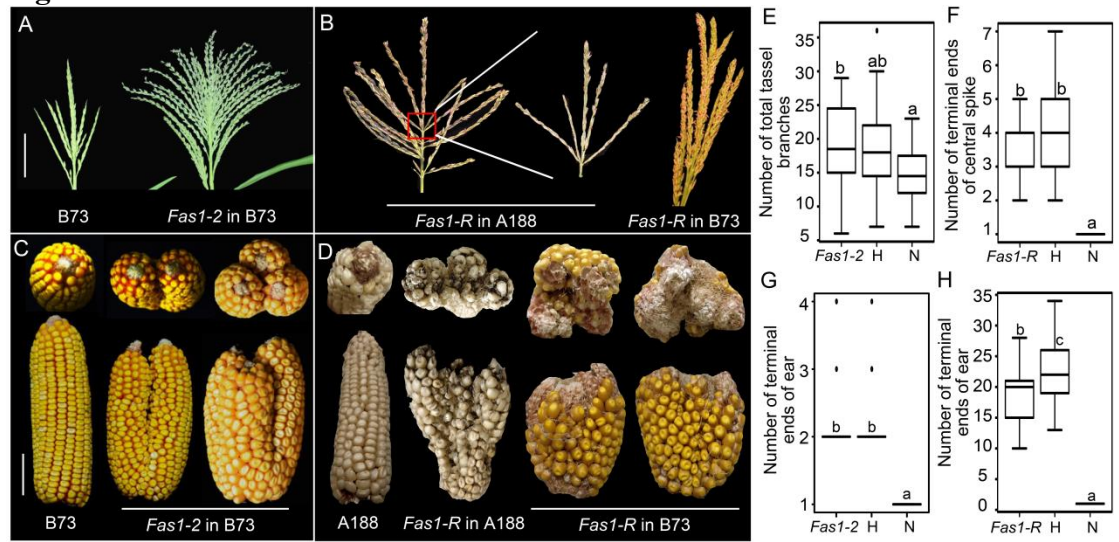


Fig. 1 Inflorescence architecture of Fas1 mutants.

- (A-B) Tassels of Fas1-2 and Fas1-R in B73 or A188. Bar=5 cm.
- (C-D) Ear bifurcations of Fas1-2 and Fas1-R in B73 or A188. Bar=5 cm.
- (E-F) Statistical analysis of the number of tassel branches or terminal ends of the central rachis of Fas1-2 in B73. Fas1-2 and Fas1-R refer to Fas1-2/Fas1-2 and Fas1-R/Fas1-R homozygotes, respectively; H refers to Fas1-2/+ or Fas1-R/+ heterozygotes; N refers to the non-mutant sibling.
- (G-H) Box and whisker plots of ear bifurcations for Fas1-2 in B73, differences in letter designations denote differences in means as measured by Student's t test, p<0.05. Genotype designations as in (E-F).

808 Figure 2.

809

810

811 812

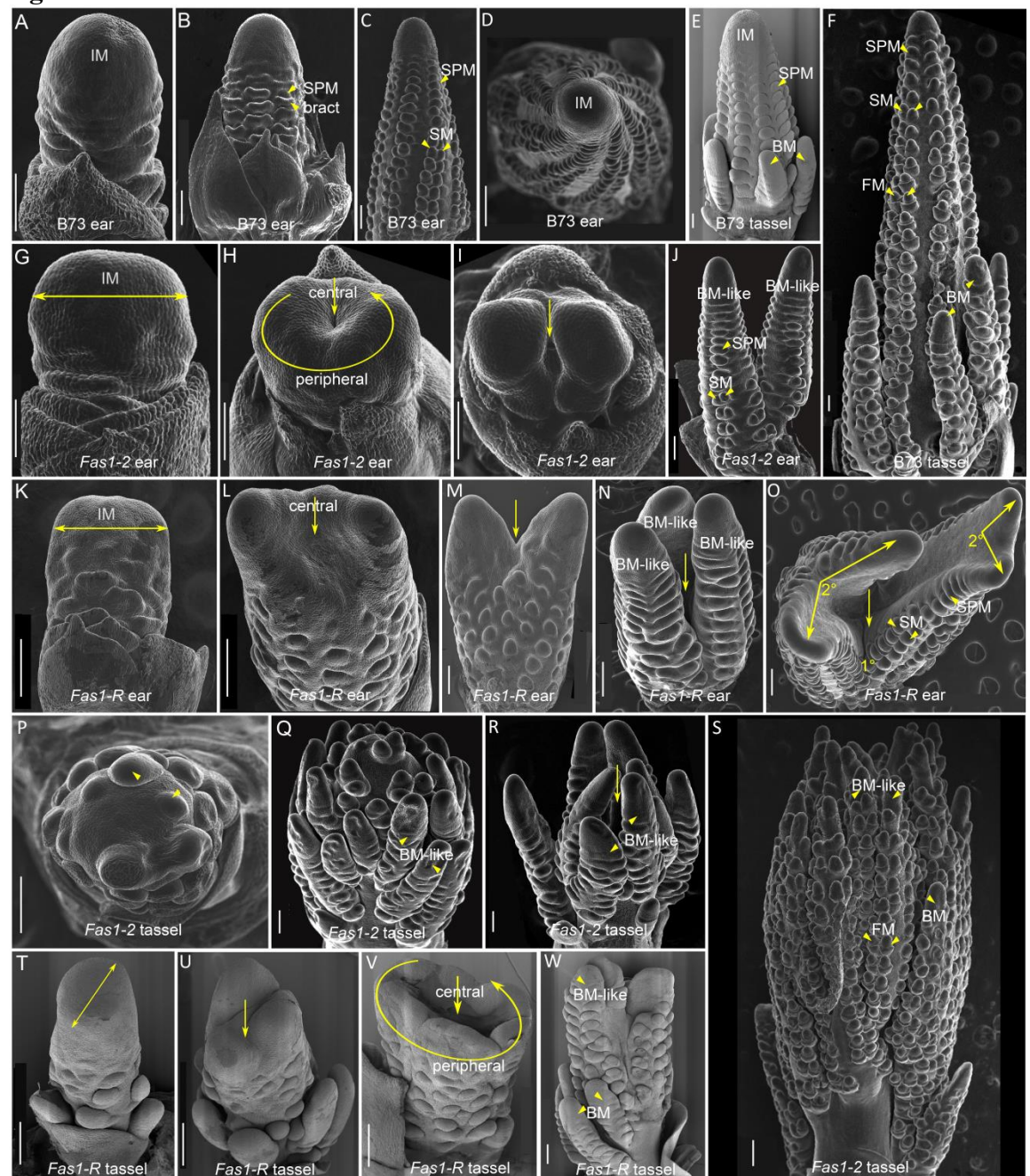


Fig. 2. Inflorescence developments in Fas1 mutants.

- (A-F) Ear and tassel development in wild type (B73).
- (G-J) Ear development in *Fas1-2*, double arrow segment in (G) marks increased IM diameter, arrows and arcs in (H) and (J) mark central/peripheral axis, respectively.
- 814 (K-O) Ear development in Fas1-R, double arrow segment in (K) marks increased IM diameter, arrows
- in (L), (M) and (N) mark central axis, 1° and 2° in (O) refers to primary and secondary bifurcations.
- 816 (P-S) Tassel development in Fas1-2, arrows in (P) refers to branch meristem primordia.

- 817 (T-W) Tassel development in Fas1-R, double arrow segment in (T) mark increased IM diameter, arrows
- 818 in (U) and (V) mark central axis, arcs in (V) mark peripheral axis. IM, inflorescence meristem; BM,
- branch meristem; SPM, spikelet pair meristem; SM, spikelet meristem; FM, floral meristem.
- 820 Bar = 200 μm

Figure 3.

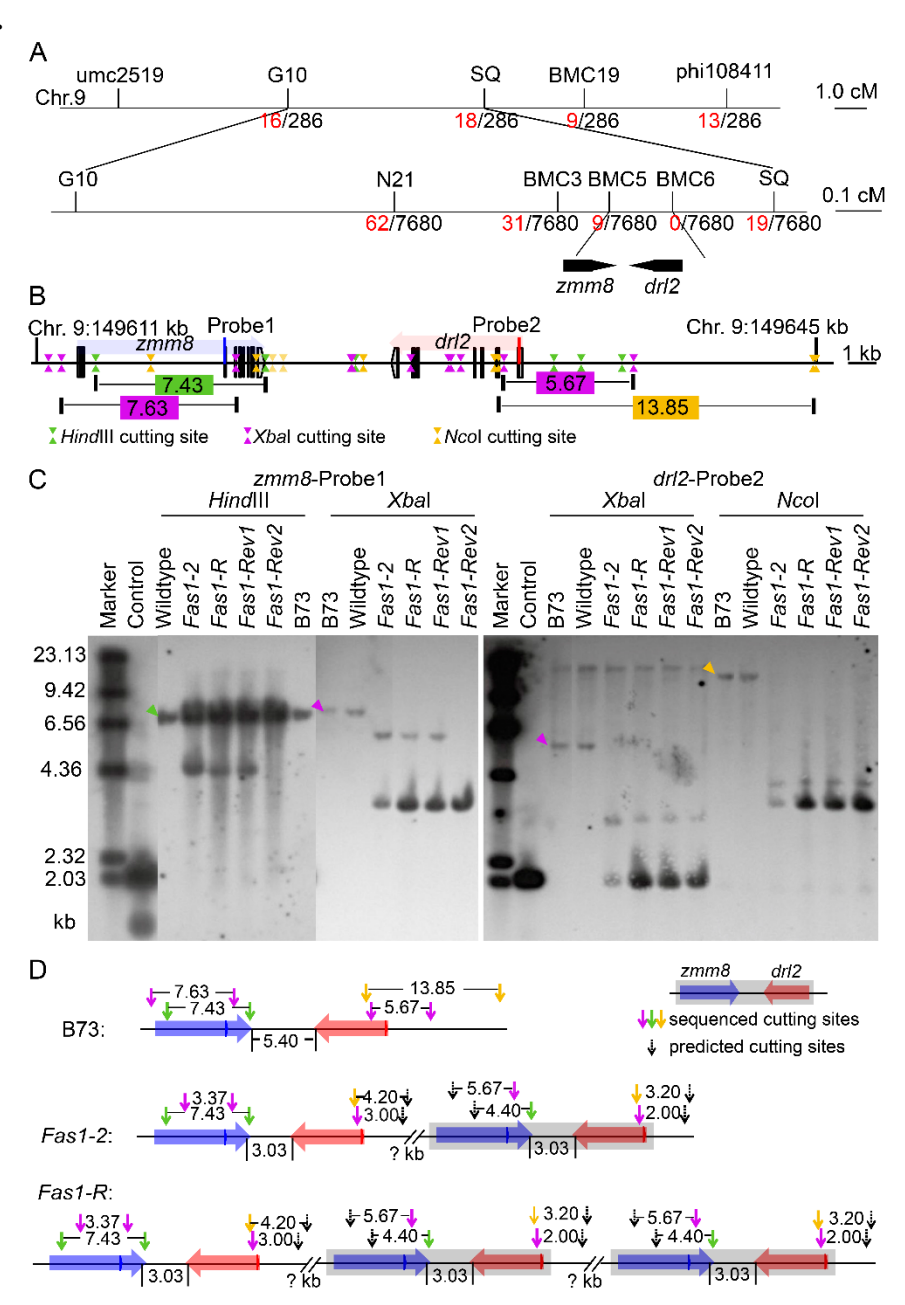


Fig. 3. zmm8 and drl2 genes are responsible for the fascicled inflorescences

(A) Genetic mapping of Fas1-2 and Fas1-R. The black markers were used for genetic mapping in a Fas1-2 F2 population, colored and black numbers show the numbers of recombinants and the population sizes. The Fas1 locus, flanked by BMC5 and BMC6, delineated a 160-Kb region on Chr9 (B73 RefGen_v4) containing two annotated genes: zmm8 and drl2.

(B) Genomic structure of *zmm8* and *drl2* in a 35-kb genomic region. Green, purple and yellow triangles refer to the site of *Hind*III, *Xba*I and *Nco*I restriction enzymes, respectively. Numbers in the boxes show the distance of two closest cut sites of each enzyme (kb). Blue and red lines refer to *zmm8* and *drl2* specific probes.

(C) DNA blot with zmm8-specific probe1 and drl2-specific probe2 using digested genomic DNA of B73, wild type, Fas1-2, Fas1-R, Fas1-Rev1 and Fas1-Rev2. Triangles refer to the bands expected in the B73 RefGen_v4genome when digested by each enzyme.
(D) Possible arrangement of zmm8 and drl2 in Fas1-2 and Fas1-R. Blue and red boxes refer to zmm8 and drl2. Arrows with pink, green and yellow color refer to sequence-defined cutting sites, and black

arrows show the predicted cutting site. The numbers showed the physical distance (kb).

837

839 Figure 4.

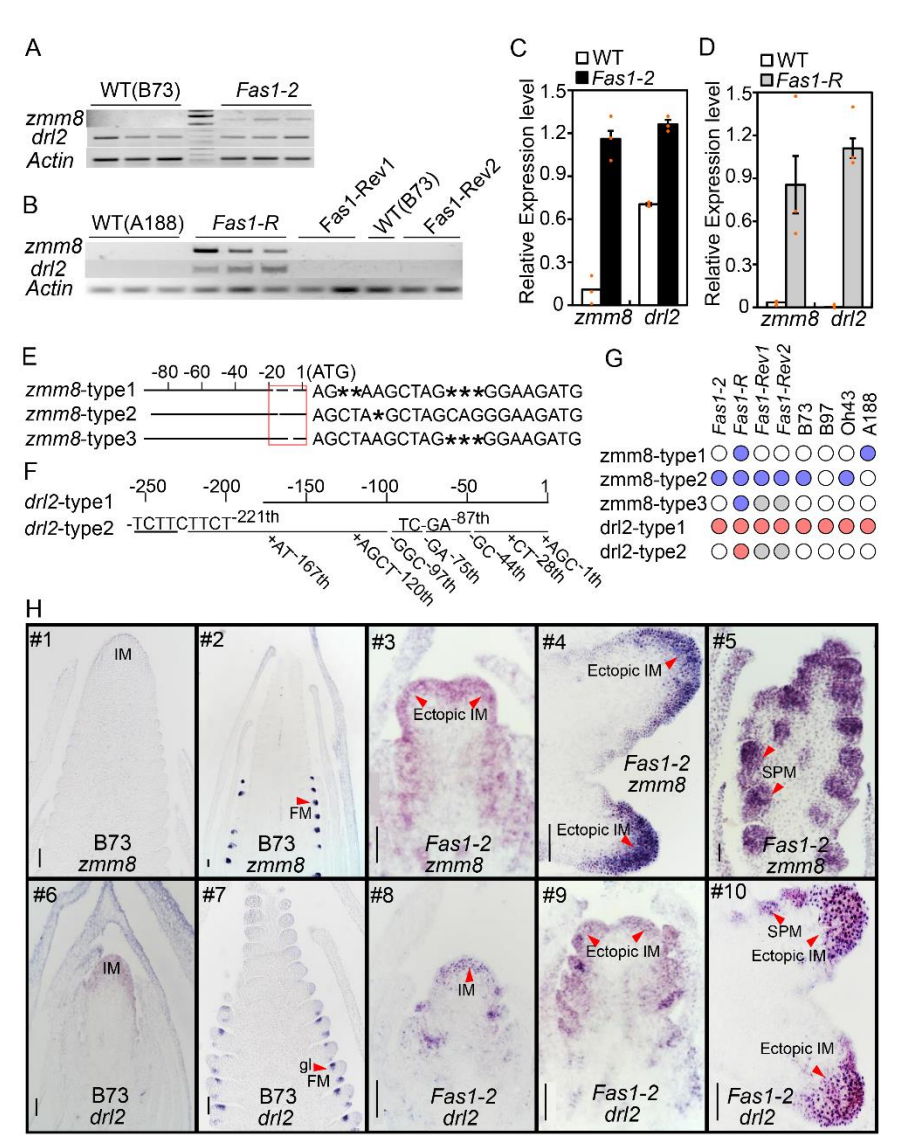


Fig. 4. zmm8 and drl2 transcripts are misexpressed in Fas1.

- (A) RNA expression analysis of *zmm8* and *drl2* in 1-2 mm ears of *Fas1-2* by RT-PCR.
- 843 (B) RNA expression analysis of *zmm8* and *drl2* in 2-3 mm ears of *Fas1-R, Fas1-Rev1*, *Fas1-Rev2* and the wild type (B73) by RT-PCR.
 - (C-D) qRT-PCR of the same samples presented in (A-B). Values are means \pm SE (n = 3).
 - (E) Three types (zmm8-type1, zmm8-type2, zmm8-type3) of 5'UTR sequence of zmm8 in Fas1-R heterozygotes identified by 5'RACE. Sequence variations in the red box located at 1 to -20, upstream of ATG. Star denotes absence of base compared to other aligned sequences.
 - (F) Two types (drl2-type1 and drl2-type2) of 5'UTR sequence of *drl2* in *Fas1-R* heterozygotes identified by 5'RACE. Sequence variations in the red boxes located at 1 to -250, upstream of the ATG.
 - (G) Presence and expression of different types of *zmm8* and *drl2* transcripts. Blue and red circles stand for *zmm8* and *drl2* sequences that are present and expressed, respectively; Gray circles stand for sequences that are present but not expressed; empty circles represent sequences that were not present.

(H) mRNA *in situ* hybridization pattern of *zmm8* and *drl2* in B73 and *Fas1-2* ear. Arrow-heads in (#2) point to the FM, in (#3, #4, #9, #10) point to ectopic inflorescence meristems, in (#5) to SPM, in (#7) indicate glume primordia (gl). Bar=100 μ m.

858 Figure 5.

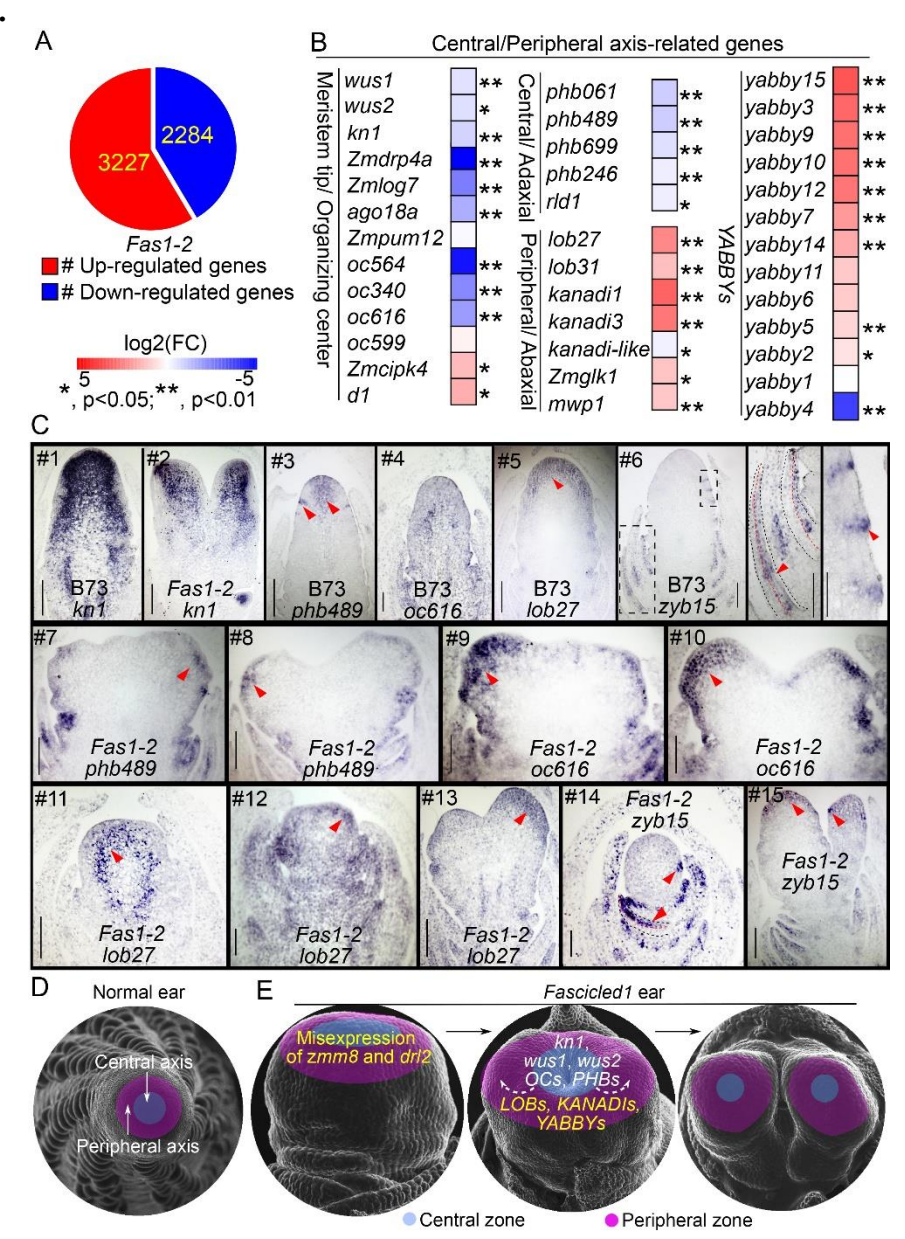


Fig. 5. Central/peripheral cell fate of inflorescence meristem in *Fas1*.

- (A) Differentially expressed genes (DEGs) detected by RNA sequencing in 1-2 mm ear of Fas1-2 allele with three biological replicates (P<0.05).
- (B) DEGs that regulate central/peripheral cell fate in RNA sequencing data. *, P<0.05, ***, P<0.01.
- (C) *in situ* hybridizations showed expression pattern of *kn1*, *phb489*, *oc616*, *lob27*, and *zyb15*, in ear primordia of wild type and *Fas1-2*. Arrow-heads point to central and SPM boundary region of normal ear in #3, to apical meristem in #5, to adaxial side of young leaf in #6 (middle) and #14 (lower arrow), to lateral organs (right) in #6, #14 (upper arrow) and #15 (lower arrow), to peripheral region of ectopic inflorescence meristem in #7-10, #12-13. Bar=100 μm.
- (D-E) Model of *zmm8* and *drl2* misexpression causing a fascicled inflorescence. Maize inflorescences are radially symmetrical, containing a single central/peripheral axis. Duplications of *zmm8* and *drl2* in

Fas1 cause their misexpression in the apical meristem of Fas1 inflorescences at the transition stage, down-regulating meristem central specific genes including kn1, wus, OCs and PHBs, and up-regulating meristem peripheral specific genes including LOBs, KANADIs and YABBYs (E), which leads to suppression of the meristematic activity of the central cells and promotion of the meristematic activity of the peripheral cells, resulting in repeatedly bifurcated inflorescences. Yellow and white color of the words in (E) marker the up- and down-regulated genes, and the arrow-heads showed the signal moved from the middle to the peripheral region of the meristem.

Fig. S1.

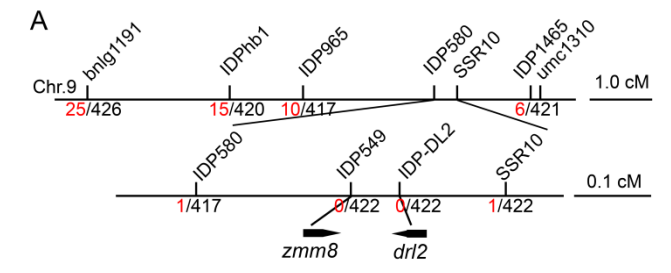


Fig. S1. Mapping of Fas1-R in A188.

(A) Genetic mapping of Fas1-R in a Fas1-R×A188 BC-6 population. Number with red and black color is the number of recombinants and the population size, respectively. Two markers (IDP580 and SSR10) flank the Fas1 mapping region on Chr9 (B73v4) containing two annotated genes: zmm8 and drl2.

885 Fig. S2.

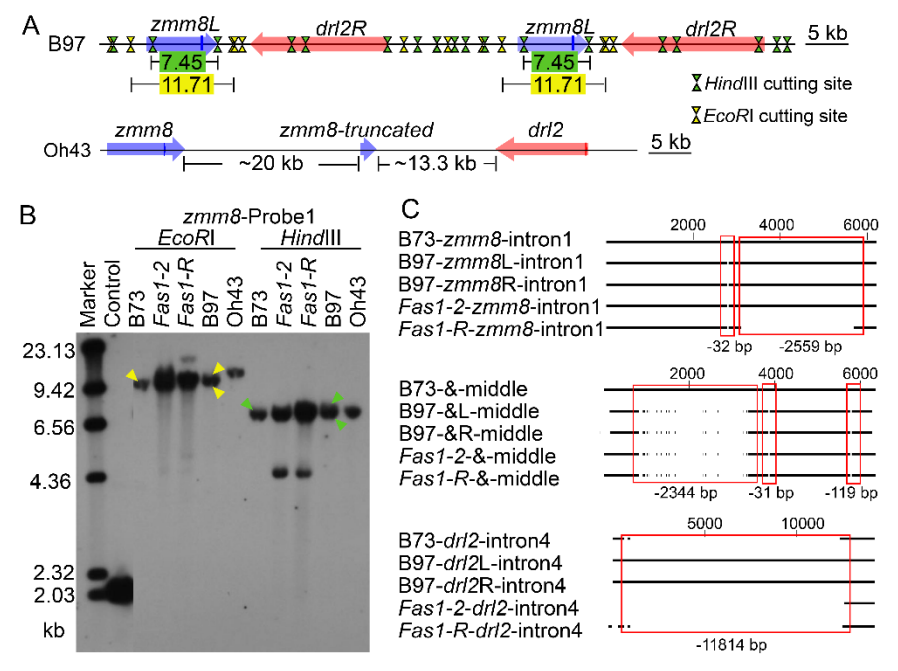


Fig. S2. zmm8 and drl2 copy number and sequence variation.

- (A) Arrangements of *zmm8* and *drl2* on Chr9 of inbred line B97 and Oh43, the blue and red boxes show copies of *zmm8* (*zmm8L* and *zmm8R* in B97, *zmm8* and *zmm8*-truncated in Oh43) and *drl2* (*drl2L* and *drl2R* in B97, *drl2* in Oh43), respectively. Green and yellow triangles refer to the site of *Hind*III and *EcoRI* restriction enzymes, respectively. Numbers in the boxes show the distance of two closest cut sites of each enzyme (kb). Blue lines refer to *zmm8* specific probe.
- (B) DNA blot with *zmm8*-specific probe1 using digested genomic DNA of B73, *Fas1-2*, *Fas1-R*, B97 and Oh43. Triangles refer to the bands expected in the B73 V4-ref or B97 genome when digested by each enzyme.
- (C) Genomic variation of one copy of *zmm8* and *drl2 in* B73, *Fas1-2*, *Fas1-R* and B97, red frames and the numbers show big deletions in *zmm8* intron1, the intergenic region between *zmm8* and *drl2*, and *drl2* intron4 that sequenced in *Fas1-2* and *Fas1-R*, compared to B73 or B97.

Fig. S3.

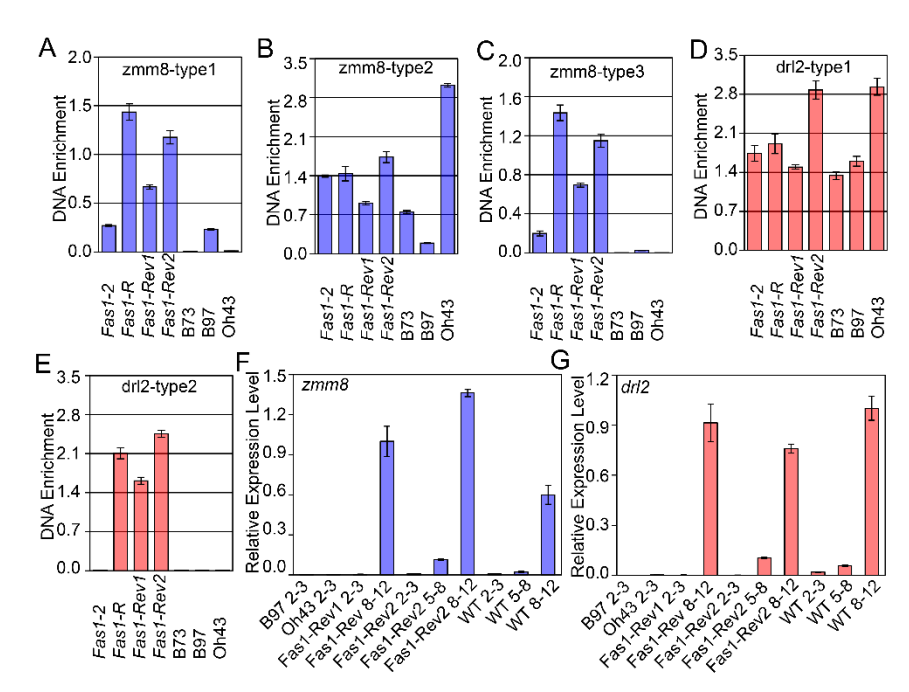


Fig. S3. DNA enrichment of different types of 5'UTR sequence and expression pattern of *zmm8* and *drl2* in different alleles.

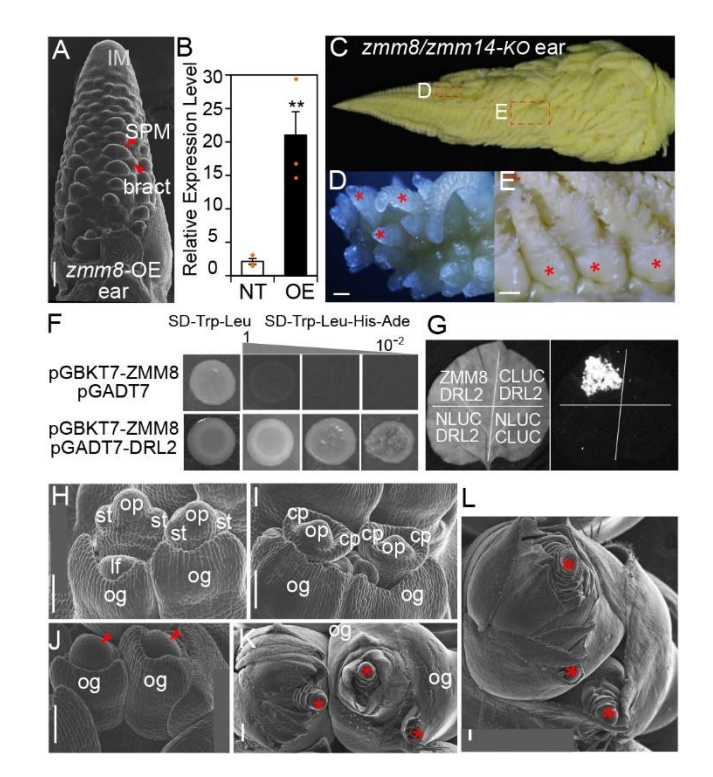
(A-E) DNA enrichment of different types of 5'UTR sequence of *zmm8* and *drl2* identified by qPCR, maize *beta-actin* (NM 001155179) gene was used as the internal control.

(F-G) mRNA relative expression patterns (RT-PCR) of *zmm8* and *drl2* in multiple ear stages of B97, Oh43, *Fas1-Rev1*, *Fas1-Rev2* and wild type (B73). The unit of the number is "mm", showing the immature ear inflorescence stages.

909 Fig. S4.

910

911



912 Fig. S4. ZMM8 overexpression, loss of function, and interaction with DRL2.

- (A) The immature ear of *zmm8* overexpression line (*zmm8*-OE) with ubiquitin promoter.
- 914 (B) zmm8 expression level in 3-5 mm ear of zmm8 non-transgenic line (NT) and overexpression line
- 915 (OE) with three biological replicates. Values are means \pm SE (n = 3). **, P<0.01.
- 916 (C-E) Female inflorescence of *zmm8/zmm14* knockout homozygous mutants (*zmm8/zmm14*-KO). Red stars point to the indeterminate branches. Bar=200 μm.
- 918 (F-G) Physical interaction of ZMM8 and DRL2 detected by yeast two hybrid and luciferase complementation image assays.
- 920 (H-I) Organogenesis from normal floral meristem of maize. lf = lower floral meristem, og = outer glume, 921 st = stamen, cp = carpel primordium, op = ovule primordium.
- 922 (J-L) Floral meristem of *zmm8/zmm14* knockout homozygous mutants (*zmm8/zmm14*-KO). Red 923 arrowheads point to the meristems that develop into indeterminate branches, red stars point the 924 indeterminate branches. Organs initiated are glumes.
- 925 If, lower floret; st, stamen; op, ovule primordium; cp, carpel primordia; og, outer glume.

927 Fig. S5.

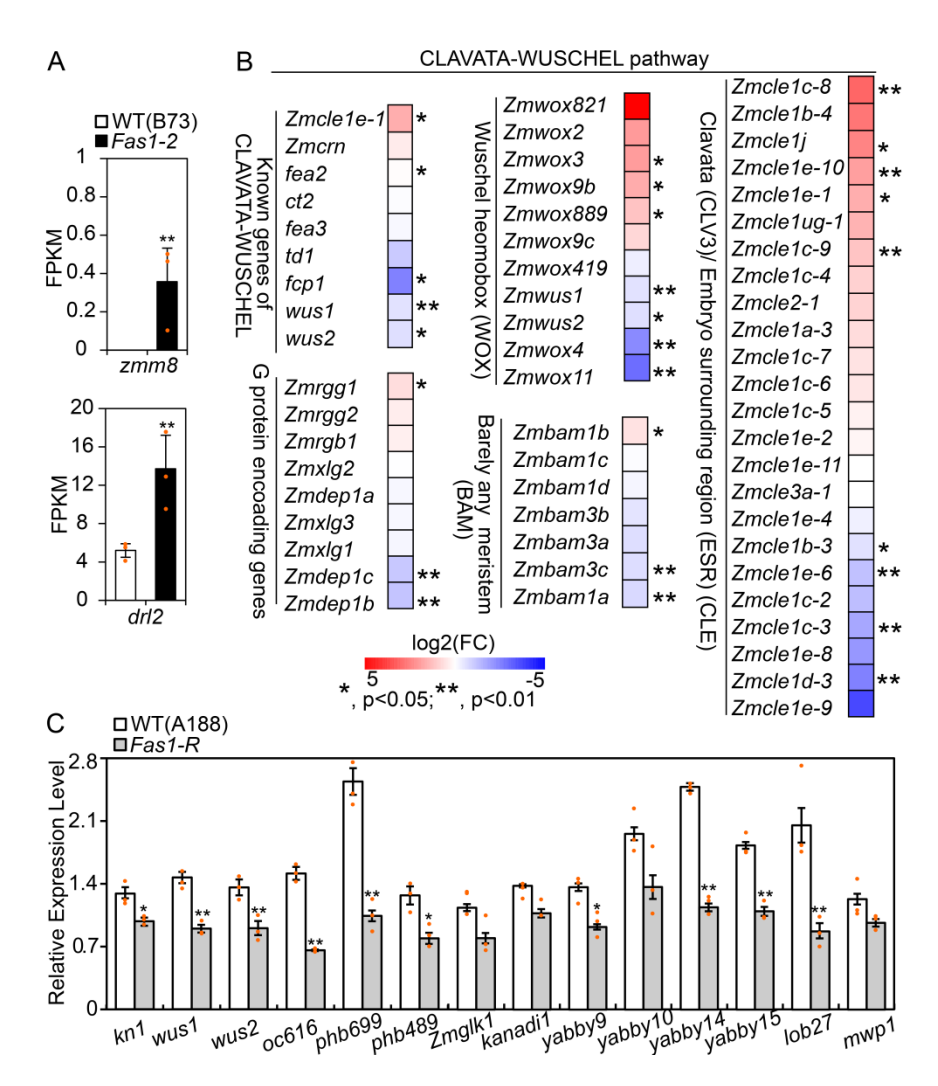


Fig. S5. Differentially expressed genes in the CLAVATA-WUSCHEL pathway and qPCR identification in *Fas1-R* allele

- (A) FPKMs value of zmm8 and drl2 in Fas1-2 RNA-seq data;
- (B) DEGs of the CLAVATA-WUSCHEL pathway in RNA-seq data.
- (C) qPCR identification of DEGs on regulating adaxial/abaxial cell fate using 2-3 mm ear of Fas1-R allele with three biological replicates. Values are means \pm SE (n = 3)
- 935 *, P<0.05, **, P<0.01.

928

929

930 931

932

933

Table S1. Tassel phenotypes in the *Fas1* allele under different backgrounds

Allele (Background)	Genotype	Sample size	Number of branches	p-value (F/N,H/N,F/H)	Number of terminal rachis points	p-value (F/N,H/N,F/H)	Tassel length	p-value (F/N,H/N,F/H)	Central rachis length	p-value (F/N,H/N,F/H)
	Fas1-R/Fas-1R	24	11.96±2.60	0.00	1.05±0.21	0.33	29.69±2.16	0.00	21.65±1.84	0.10
Fas1-R (A188)	Fas1-R/+	25	17.42±3.01	0.02	1.23±0.43	0.01	29.54±2.14	0.00	20.74±2.39	0.00
	+/+	19	19.10±1.65	0.00	1.00±0.00	0.06	22.11±1.68	0.84	22.6±1.44	0.11
	Fas1-R/Fas1-R	20	7.35±1.66	0.45	3.60±0.75	0.00	23.79±3.64	0.00	15.33±3.25	0.00
Fas1-R (B73)	Fas1-R/+	21	8.00±1.18	0.58	4.00±1.26	0.00	25.24±3.88	0.01	16.38±3.02	0.00
	+/+	20	7.75±1.65	0.16	1.00±0.00	0.23	28.19±3.27	0.22	20.45±2.61	0.29
	Fas1-2/Fas1-2	36	23.15±3.38	0.00	nd		nd		nd	
Fas1-2 (B73)	Fas1-2/+	80	18.23±5.37	0.00	nd		nd		nd	
	+/+	60	14.48±3.66	0.60	nd		nd		nd	

Values are means \pm s.d., *p*-value is calculated by a Student's t-test.

p-value (F/N, H/N, F/H) of each phenotype refer to p-value in Fas1/Fas1 compared to +/+, Fas1/+ to +/+ and Fas1/Fas1 to Fas1/+, respectively.

Table S2. Ear phenotypes in the *Fas1* allele under different backgrounds

Allele (Background)	Genotype	Sample size	Number of terminal ends	p-value (F/N,H/N,F/H)	Kernel row number	p-value (F/N,H/N,F/H)	Length-width ratio	p-value (F/N,H/N,F/H)
	Fas1-R/Fas1- R	24	3.63±1.38	0.00	27.5±5.57	0.00	0.34±0.04	0.00
Fas1-R (A188)	Fas1-R/+	25	3.01±0.98	0.00	21.31±3.58	0.00	0.38 ± 0.04	0.00
	+/+	19	1.05±0.22	0.04	14.5±5.73	0.00	0.54 ± 0.05	0.00
	Fas1-R/Fas1- R	20	18.55±4.26	0.00	52.8±11.17	0.00	0.24±0.02	0.00
Fas1-R (B73)	Fas1-R/+	21	21.67±5.13	0.00	56.95±8.14	0.00	0.23 ± 0.01	0.00
	+/+	20	1.00±0.00	0.18	17.8±1.28	0.04	0.47 ± 0.03	0.09
	Fas1-2/Fas1-2	36	2.05±0.22	0.00	nd		nd	
Fas1-2 (B73)	Fas1-2/+	80	2.08±0.31	0.00	nd		nd	
	+/+	60	1.00±0.00	0.23	nd		nd	

Values are means \pm s.d., *p*-value is calculated by a Student's t-test.

p-value (F/N, H/N, F/H) of each phenotype refer to p-value in Fas1/Fas1 compared to +/+, Fas1/+ to +/+ and Fas1/Fas1 to Fas1/+, respectively.

1 Table S3. Primers used in the paper

	primer name	genome location (B73- V4)/Gene ID	Forward/Reverse primer sequence (5'-3')
	umc2159	chr9:145088582145088519	F-GTAGTACGACATGGCTGGCTGG
			R-CTCACCAGTGCTCGCTCACTTT
	G10	chr9:147312600147313051	F-GACTTGTGCATATTCTGGATC
			R-AATGCGATTAGACTGGGAAT
	N21	chr9:148211566148458979	F-ACATGTGGAAGGGTCATGGG
			R-AGCAATAGTGGCTCAACGGA
primers for	BMC3	chr9:149403624149403646	F-ACATGTGGAAGGGTCATGGG
fine mapping in			R-AGCAATAGTGGCTCAACGGA
Fas1-2X B73 F2	BMC5	chr9:149615440149615831	F-TCGTGGCAAAACTCTAATTCTAAA
population			R-TGACGGTACAAGCTCTCTGTG
	BMC6	chr9:149784788149784812	F-TCCAGATTTCTTCCTACCCAAA
			R-TTGTCAGCGAGTCAAAATCG
	SQ	chr9:150633475150633500	F-GCCTACCCCAACTTGATTGA
			R-GGCTATCAAATCCGTCTCCA
	BMC19	chr9:151546822151547206	F-AGCTCCTCAAATCCCTTTGG
			R-AGGCCGGTTATTTTCTTCC
	phi108411	chr9:154421898154422020	F-CGTCCCTTGGATTTCGAC
			R-CGTACGGGACCTGTCAACAA
	bnlg1191	chr9:147741889147742084	F-AATCATGCGTAGGCGTAGCT
			R-GCCAGAGGAAAAAGAAGGCT
primers for fine	IDPhb1	chr9:148185585148186016	F-CTCTTCCTCCGCTACGACAC
mapping in Fas1-RX			R-TCGTGAAGTCGTTGCTCATC
A188 backcross	IDP965	chr9:148926232148926698	F-CCAGACGTGACAACCATGAC
population			R-ACGAATGTCAGCTGCTCGAT
	IDP580	chr9:149600769149600777	F-TGACAAGTTTGGACGGACCTCTTC
			R-TTCTGTCTGCTCAGGAGAAGAGGT
	IDP549	chr9:149621309149621329	F-GAAGCCCAGAAATGAAGACG

	-		R-GAAGCCCAGAAATGAAGACG
	SSR2	chr9:149613728149613663	F-AAACGTGCTCAAAGTGAAAGC
			R-GGAGAGCACCTGAACTTTGG
	DP_DL2	chr9:149627639149628051	F-ACATGCTCCTTGGCCCTATC
			R-CGAAGCCAGATATCCCTCAC
	SSR6	chr9:149715622149715436	F-TGTCGGCTCAACGACAATAG
			R-GCACAAACGCATTCAATCAG
	SSR10	chr9:149768405149768557	F-CAAAAATCTAGGCTGCTACCG
			R-TTAGATTGGATGCTCCTCTGC
	IDP1465	chr9:149915500149914633	F-ATGGGAGAGGAACACAAACG
			R-ATCGTTTAAGCCCACAATGG
	umc1310	chr9:149952577149952694	F-GAGGAAGAGTTGGCCAGGATG
			R-AACTCCGAGATCTACGACAACAGC
	zmm8 southern	Zm00001d048082	F-AGGATGACGATTGAGCTCTCG
primers for southern			R-GCACAAGGCAATCAAAGTGA
blot	ZmDL2 southern	Zm00001d048083	F-GTGGCCGGCCGTACGTG
			R-CGGTCTCCTCCCCTTTCTT
	ZMM8- 4F/ZMM8-4R	Zm00001d048082	F-CTCCAACTACAGCACACAGGAA
primers for			R-CTAATCGTTGGTGCAGTTTCAA
RT-PCR	drl2_F11/drl2_R9	Zm00001d048083	F-AGCCAGATATCCCTCACAGG
			R-GCGTACAATCCAACAAGAGC
	ACTIN-F/R	Zm00001d010159	F-TACGAGATGCCTGATGGTCAGGTCA
			R-TGGAGTTGTACGTGGCCTCATGGAC
	ZMM8- 5F/ZMM8-5R	Zm00001d048082	F-AAACAAGTCCGCAGAATGTGA
primers for Q-PCR			R-CCATTACAATCAGGCAGCTAATC
	drl2_F11/drl2_R9	Zm00001d048083	F-AGCCAGATATCCCTCACAGG
			R-GCGTACAATCCAACAAGAGC
	QKN1	Zm00001d033859	F-ACCTGAAGCAGATCAACAACTG
	=		

		R-GAACCATTAGTCTTTATAGCTAGGC
QWUS1	Zm00001d001948	F-AAGGAGTAGTGGCTAGTGACCAAC
		R-ACACTATTGCCTTCACTCACACAT
QWUS2	Zm00001d026537	F-CCCGAGACACTCCCTCTTT
		R-CACCCCAGAACGGCAAGTAG
QZYB14	Zm00001d025944	F-TTCTCCGGCTGGGATAGACA
		R-CGCGGAATGGTCTATAGCGT
QZYB10	Zm00001d032502	F-CGGGCTACTAAAGGAAGGGC
		R-CAGCCTACCAAACACGTCCA
QZYB15	Zm00001d017391	F-CTTGATGCGCGCTCTAACTTG
		R-CAGCAGCCAACATGGGCATC
QZYB9	Zm00001d013895	F-GGCTTCTTAAGGAAGGGCTC
		R-CAGCAGCCAACATGGGCATC
QGLK55	Zm00001d024532	F-CTCCGTCTTAACACGATCCCA
		R-GTGCCAGCGAGTTGAACCT
QMWP1	Zm00001d020384	F-TTGCTGCTGCTGTACTT
		R-TAGCTGCTAGCCATGCGTC
QGLK1	Zm00001d039260	F-CGCCACCGGATGACATACTA
		R-TAGCAGATCTGTGTCAAGCTCC
QPHB699	Zm00001d013699	F-GAAGGTCCTGAGCGACGAC
		R-AAAGGCAAGAGCGACCAGTA
QLOB27	Zm00001d042560	F-GCCTAGTTGGAGGCGGTAAT
		R-ACTAAGTGGATCGAGCCTGC
kn1-F1		CCCAAACCCTTTTCCTCTTTCCC
kn1-R1	kn1	CTCGAGGTAGGCAGTGAGGA
kn1-F2	F1/R1: 5'UTR probe 518bp	ACCTCGAGTGCAACAAGGTG
kn1-R2	F2/R2: HD box probe 642bp	CCATCATCAGGTGGTGCATC
kn1-F3	F3/R3: 3'UTR probe 416bp	GTACCACCACCAATGC
kn1-R3		GATTAGGCAGAAACTAGC

	ZMM8- 5F/ZMM8-5R	Zm00001d048082	F-AAACAAGTCCGCAGAATGTGA				
			R-CCATTACAATCAGGCAGCTAATC				
	drl2_F11/drl2_R9	Zm00001d048083	F-AGCCAGATATCCCTCACAGG				
			R-GCGTACAATCCAACAAGAGC				
	ILOB27	Zm00001d042560	F-GCATCAGCCCGTTCTTGAAGT				
primers for			R-CGTACGGATCGGAGCCTAGT				
in situ	IPHB-498	Zm00001d041489	F-GTTCGCGTATCGAACTGAAGC				
			R-ACGTAGTAGGGCAAAAGGCG				
	IOC616	Zm00001d021616	F-CGCTCCCTGTTTCTCTGTCT				
			R-AAAAGAAGCCACCCCGTACT				
	IZYB15	Zm00001d017391	F-AATCAGTGGGCCCATTTCCC				
			R-ACAGATGTTCAACTTGTTCTCCA				
	ZMM8–NLUC	F-CGAGCTCGGTACCCGGGATCCATGGGTCGCGGCAAGGTGGAGC					
	ZIVIIVIO IVECE	R-CGCGTACGAGATCTGGTCGAC GCTGGTCCATGTAGGCCGT-3'					
	DRL2-CLUC	F-TACGCGTCC	CCGGGGCGGTACC ATGGATACGGTTTCACAGTC				
primers for protein-	DREZ CEGC	R-ACGAAAGC	TCTGCAGGTCGAC CTAGATGTTGCGCTCAATCT				
protein analysis	pGBKT7–ZMM8	F-TAGGCCATGGAGGCCGAATTC ATGGGTCGCGGCAAGGTGGAGC					
	pobki /-Ziviivio	R-CCGCTGCAGGTCGACGGATCC TCAGCTGGTCCATGTAGGCCGT					
	pGADT7–DRL2	F-GCCATGGAGGCCAGTGAATTC ATGGATACGGTTTCACAGTC					
	poad17-bkt2	R-CAGCTCGAGCTCGATGGATCC CTAGATGTTGCGCTCAATCT					
	Z8GSP1-R	Zm00001d048082	R-CATTACAATCAGGCAGCTAATCGTTGGT				
primers for	Z8GSP2-R	Zm00001d048082	R-TCGTGGATCACATTCTGCGGACTTGTTT				
5' RACE	ZDL2GSP1-R	Zm00001d048083	R-AAGGGTGCGTACAATCCAACAAGAGCAA				
	ZDL2GSP2-R	Zm00001d048083	R-GTGAGGGATATCTGGCTTCGCAGCTTTG				
zmm8	gRNA1	Zm00001d048082	GGATCGAGAACAAGATCAGCCGG				
gRNA	gRNA2	Zm00001d048082	GTCGCGCTCATCATATTCTCCGG				
zmm8	gRNA1	Zm00001d028217	GCTTGGCGAACGTCACCTGGCGG				
gRNA	gRNA2	Zm00001d028217	GCTTCAGAGATATCTCTATTTGG				
primers for DNA	ZDL2GSPtc1-1	Zm00001d048083	F-ACAGCCAGACACGCGCTGCT				
enrichment	_		R-CTGCGAAACCATATCCATGC				

ZDL2GSPtc2-2	Zm00001d048083	F-GCTAGCTGATTTCCGATCTC
		R-ACTGTGAAACCGTATCCATGC
Z8GSPtc1	Zm00001d048082	F-ACAAGCAGAAGCTAGGGAAG
		R-TTCTTGAGCAGCCCGTTCCT
Z8GSPtc2	Zm00001d048082	F-ACAAGCAGCTAGCTAGCAGG
		R-TTCTTGAGCAGCCCGTTCCT
Z8GSPtc3	Zm00001d048082	F-ACAAGCAGCTAAGCTAGGGA
		R-TTCTTGAGCAGCCCGTTCCT

Table S4. Differentially expressed genes in the RNA-seq data used in Fig.5 and Fig. S5

Gene ID	Annotation	FPKM in Fas1-2	FPKM in WT	log2	<i>p</i> -value
Zm00001d017391	yabby 15	280.09	50.17	2.48	0.00
Zm00001d018829	yabby 3	4.61	1.00	2.20	0.00
Zm00001d013895	yabby 9	84.64	20.24	2.06	0.00
Zm00001d032502	yabby 10	84.24	20.19	2.06	0.00
Zm00001d033508	yabby 12	4.00	0.00	2.00	0.00
Zm00001d048083	yabby 7	15.81	5.68	1.48	0.00
Zm00001d025944	yabby 14	80.17	34.24	1.23	0.00
Zm00001d031109	yabby 11	1.24	0.72	0.79	0.15
Zm00001d013661	yabby 6	6.81	4.00	0.77	0.11
Zm00001d041277	yabby 5	3.11	2.03	0.62	0.00
Zm00001d028216	yabby 2	3.12	2.33	0.42	0.02
Zm00001d002829	yabby 1	6.20	6.22	(0.01)	0.11
Zm00001d021863	yabby 4	0.41	5.08	(3.65)	0.00
Zm00001d031061	phb061	20.22	39.14	(0.95)	0.00
Zm00001d041489	phb489	58.64	105.78	(0.85)	0.00
Zm00001d013699	phb699	87.39	133.29	(0.61)	0.00
Zm00001d033246	phb246	124.95	154.48	(0.31)	0.00
Zm00001d048527	rld1	65.24	87.55	(0.42)	0.03
Zm00001d001948	wus1	2.57	4.60	(0.84)	0.01
Zm00001d026537	wus2	3.08	4.70	(0.61)	0.01
Zm00001d033859	kn1	105.28	187.82	(0.84)	0.00
Zm00001d042560	lob27	35.38	10.63	1.73	0.00
Zm00001d012180	lob31	6.31	3.31	0.93	0.00
Zm00001d032249	kanadi l	4.00	0.84	2.26	0.00
Zm00001d050350	kanadi3	1.95	0.49	1.99	0.00
Zm00001d024532	kanadi-like	25.02	29.67	(0.25)	0.03
Zm00001d039260	zmglk1	32.98	18.22	0.86	0.01
Zm00001d020384	mwp1	16.14	9.10	0.83	0.06

Zm00001d028495	zmdrp4a	13.74	0.47	(4.88)	0.00
Zm00001d044327	zmlog7	28.33	5.12	(2.47)	0.00
Zm00001d006351	ago18a	2.20	0.75	(1.55)	0.01
Zm00001d052953	zmpum12	6.46	6.01	(0.10)	0.38
Zm00001d021616	oc616	146.95	39.62	(1.89)	0.00
Zm00001d002564	oc564	11.29	0.50	(4.50)	0.00
Zm00001d008340	oc340	1.22	0.26	(2.26)	0.00
Zm00001d016599	oc599	58.92	67.67	0.20	0.48
Zm00001d033316	zmcipk4	0.81	1.61	1.00	0.04
Zm00001d039634	d1	4.17	9.41	1.17	0.01
Zm00001d025918	zmcle1b-4	0.72	0.18	1.99	0.32
Zm00001d040003	zmcle1j	3.65	1.05	1.79	0.01
Zm00001d026498	zmcle1c-7	2.78	2.08	0.42	0.74
Zm00001d037664	zmcle1c-8	7.40	1.58	2.22	0.00
Zm00001d019092	zmcle1e-10	0.88	0.33	1.40	0.00
Zm00001d013520	zmcle1e-1	8.09	3.56	1.19	0.01
Zm00001d009202	zmcleug-1	6.73	3.12	1.11	0.05
Zm00001d014620	zmcle1c-5	4.09	3.55	0.20	0.07
Zm00001d001990	zmcle1c-4	7.46	4.69	0.67	0.47
Zm00001d051944	zmcle2-1	47.37	30.20	0.65	0.32
Zm00001d015282	zmcle1c-9	11.59	6.34	0.87	0.00
Zm00001d038680	zmcle1a-3	2.19	1.53	0.52	0.53
Zm00001d002849	zmcle1b-3	8.13	11.97	(0.56)	0.05
Zm00001d036515	zmcle1c-6	1.03	0.80	0.36	0.41
Zm00001d034507	zmcle1e-2	42.79	38.66	0.15	0.43
Zm00001d013054	zmcle1e-4	12.95	15.71	(0.28)	0.18
Zm00001d022023	zmcle1e-8	0.76	3.01	(1.98)	0.15
Zm00001d038641	zmcle1e-6	7.18	16.20	(1.17)	0.01

Zm00001d008722	zmcle1c-2	0.50	1.17	(1.24)	0.24
Zm00001d028503	zmcle1c-3	1.58	5.01	(1.66)	0.01
Zm00001d003425	zmcle1e-9	0.21	2.40	(3.49)	0.06
Zm00001d003320	zmcle1d-3	0.85	4.54	(2.41)	0.00
Zm00001d033569	zmcle1e-11	0.00	0.23	#NUM!	0.18
Zm00001d009553	zmcle3a-1	0.55	0.00	#DIV/0!	0.25
Zm00001d042821	wox821	0.33	0.03	3.70	0.07
Zm00001d042920	wox2	0.70	0.25	1.48	0.07
Zm00001d052598	wox3	5.73	2.12	1.44	0.03
Zm00001d043937	wox9b	3.32	1.43	1.22	0.02
Zm00001d004889	wox889	6.40	3.46	0.89	0.03
Zm00001d039017	wox9c	18.39	12.25	0.59	0.15
Zm00001d012419	wox2	0.23	0.29	(0.32)	0.66
Zm00001d001948	wus1	2.57	4.60	(0.55)	0.01
Zm00001d026537	wus2	3.08	4.70	(0.61)	0.01
Zm00001d026453	wox4	0.07	0.34	(2.22)	0.01
Zm00001d022524	wox11	0.26	1.78	(2.78)	0.00
Zm00001d033859	kn1	105.28	187.82	(0.84)	0.00
Zm00001d015211	zmrgg1	23.78	16.79	0.50	0.39
Zm00001d033287	zmrgg2	12.85	10.66	0.27	0.54
Zm00001d033422	zmrgb1	27.70	23.50	0.24	0.02
Zm00001d035926	zmxlg2	34.78	34.87	(0.00)	0.98
Zm00001d032072	depla	24.64	27.10	(0.72)	0.38
Zm00001d030916	zmxlg3	64.81	71.45	(0.14)	0.38
Zm00001d054088	zmxlg1	37.11	41.74	(0.17)	0.29
Zm00001d020629	dep1c	9.99	20.61	(1.04)	0.00
Zm00001d005824	dep1b	15.80	34.32	(1.12)	0.00
Zm00001d034240	zmbam1b	96.42	71.36	0.43	0.01

Zm00001d018752	zmbamlc	94.54	97.25	(0.04)	0.76
Zm00001d028317	zmbam1d	240.26	273.37	(0.19)	0.26
Zm00001d007254	zmbam3b	8.20	11.58	(0.50)	0.12
Zm00001d048968	zmbam3a	7.28	11.16	(0.62)	0.13
Zm00001d039218	zmbam3c	34.17	52.94	(0.63)	0.03
Zm00001d013162	zmbamla	16.91	27.95	(0.72)	0.00
Zm00001d013520	zmcle1e-1	8.09	3.56	1.19	0.01
Zm00001d042268	zmcrn	59.44	48.43	0.30	0.04
Zm00001d051012	fea2	52.98	51.15	0.05	0.76
Zm00001d027886	ct2	16.73	17.20	(0.04)	0.66
Zm00001d040130	fea3	17.65	19.14	(0.12)	0.57
Zm00001d014793	td1	38.97	78.39	(1.01)	0.03
Zm00001d003320	fcp1	0.85	4.54	(2.41)	0.00

Events	gene	Editing Information
ZZC01	zmm8	AGCGGATCGAGAACAAGATCAGCCGGCACCGAGGT//CGCGCTCATCATATTCTCCGGC
	zmm14	CAGCCGCCAGGTGACGTTCGCCAAGCGCCGCAAC//CTTCAGAGATATCTCTATTTGG
KO#1	zmm8	AGCGGATCGAGAACAAGATC(-98bp)CTCCGGC
	zmm14	CAGCCGC(-23bp)AAC//CTTCAGAGATATCATTTGG
KO#2	zmm8	AGCGGATCGAGAACAAG(-9bp)//CGCGCTCATCATATTCTCCGGCCGCGC
	zmm14	CAGCCGCCA(-1bp)GTGACGTTCGCCAAGCGCCGCAAC//CTTCAGAGATAT(-6bp)TTGG
KO#3	zmm8	GGG
	zmm14	CAGCCGCC(-3)TGACGTTCGCCAAGCGCCGCAAC//CTTCAGAGA-(-8bp)ATTTGG

Table S5. Editing Information of CRISPR-Cas9 knockout line

The words in red showed the gRNAs sequences; the numbers in the brackets showed the size of base pair deletions.